Electronic Supplementary Information for

Discs, dumbbells and superdiscs: molecular and supermolecular architecture dependent magnetic behavior of mesogenic Blatter radical derivatives

Szymon Kapuściński,[a] Jacek Szczytko,[b] Damian Pociecha,[c] Marcin Jasiński,[a] Piotr Kaszyński[a,d,e]*

[a] *Faculty of Chemistry, University of Łódź, Tamka 12, 91-403 Łódź, Poland*
[b] *Institute of Experimental Physics, Faculty of Physics, University of Warsaw, Pasteura 5, 02-093 Warsaw, Poland.*
[c] *Faculty of Chemistry, University of Warsaw, Żwirki I Wigury 101, 02-089 Warsaw, Poland*
[d] *Organic Materials Research Group, Centre of Molecular and Macromolecular Studies, Polish Academy of Sciences, Sienkiewicza 112, 90-363 Łódź, Poland*
[e] *Department of Chemistry, Middle Tennessee State University, Murfreesboro, TN, 37130, USA*

Table of Content:

1. Additional synthetic details.

Synthesis of 3,6-diaryl benzo[*e*][1,2,4]triazines 2[3] and 2[6]. Following a procedure for preparation of **2[1]**,[1] a solution of 6-bromobenzo[*e*][1,2,4]triazine derivative **5** [1] or **6** [2] (1.00 mmol), K_2CO_3 (516 mg, 3.73 mmol), and appropriate arylboronic acid (2.0 mmol; 4-benzyloxyphenylboronic acid for reaction with **5** to obtain **2[6]**, 3,4,5-tridodecyloxyphenylboronic acid[1] for reaction with **6** to obtain **2[3]**) in THF/H_2O (5:2 mixture, 25 mL) was degassed by a repeated procedure of freeze-pump-thaw and $Pd(PPh_3)_4$ (144 mg, 10 mol% with respect to the boronic acid) was added. The mixture was refluxed for 24 hrs, poured into water (70 mL) and extracted with CH_2Cl_2 (3 × 50 mL). Combined organic layers were dried over Na_2SO_4, and the solvents were removed under reduced pressure. The crude product was flash chromatographed (SiO_2, gradient petroleum ether/CH_2Cl_2 1:1 to pure CH_2Cl_2) and recrystallized from EtOH/EtOAc mixtures to give 3,6-diaryl benzo[*e*][1,2,4]triazine **2[n]**.

6-(3,4,5-tridodecyloxyphenyl)-3-(4-benzyloxyphenyl)benzo[*e*][1,2,4]triazine (2[3])

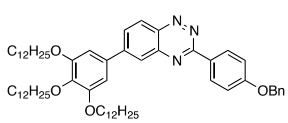

Yellow solid, yield: 914 mg (97%): mp 92−93 °C; ^{1}H NMR (600 MHz, $CDCl_3$) δ 0.88 (t, J = 7.0 Hz, 6H), 0.89 (t, J = 6.9 Hz, 3H), 1.27 – 1.41 (m, 48H), 1.52 (quin, J = 7.5 Hz, 6H), 1.80 (quin, J = 7.1 Hz, 2H), 1.87 (quin, J = 7.1 Hz, 4H), 4.05 (t, J = 6.6 Hz, 2H), 4.09 (t, J = 6.5 Hz, 4H), 5.20 (s, 2H), 6.96 (s, 2H), 7.18 (d, J = 8.9 Hz, 2H), 7.36 (t, J = 7.3 Hz, 1H), 7.42 (t, J = 7.5 Hz, 2H), 7.49 (d, J = 7.4 Hz, 2H), 8.02 (dd, J_1 = 8.8 Hz, J_2 = 1.8 Hz, 1H), 8.16 (d, J = 1.7 Hz, 1H), 8.51 (d, J = 8.8 Hz, 1H), 8.73 (d, J = 8.9 Hz, 2H); ^{13}C NMR ($CDCl_3$, 151 MHz) δ 14.3, 22.8, 26.3, 29.52, 29.56, 29.59, 29.62, 29.78, 29.82, 29.87, 29.91, 29.92, 30.56, 32.09, 32.11, 69.6, 70.3, 73.8, 106.7, 115.4, 125.4, 127.7, 128.3, 128.7, 128.8, 129.8, 129.9, 130.7, 134.0, 136.7, 139.8, 141.7, 145.6, 148.4, 153.9, 160.2, 161.8; IR (KBr) v 2919, 2850, 2363, 1606, 1468, 1384, 1334, 1274, 1133 cm^{-1}; MALDI-MS, m/z 945 (100, $[M]^+$). Anal. Calcd for $C_{62}H_{91}N_3O_4$: C, 79.02; H, 9.73; N, 4.46. Found: C, 78.96; H, 9.73; N, 4.45.

6-(3,4,5-Tridodecyloxyphenyl)-3-(4-benzyloxyphenyl)benzo[*e*][1,2,4]triazine (2[6])

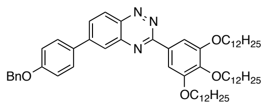 Yellow solid; yield: 801 mg (85%): mp 82−83 °C; ^{1}H NMR (600 MHz, $CDCl_3$) δ 0.88 (t, J = 7.0 Hz, 6H), 0.89 (t, J = 7.1 Hz, 3H), 1.27 – 1.42 (m, 48H), 1.52 (quin, J = 7.3 Hz, 2H), 1.54 (quin, J = 7.3 Hz, 4H), 1.80 (quin, J = 7.1 Hz, 2H), 1.89 (quin, J = 7.1 Hz, 4H), 4.10 (t, J = 6.6 Hz, 2H), 4.18 (t, J = 6.5 Hz, 4H), 5.17 (s. 2H), 7.14 (d, J = 8.7 Hz, 2H), 7.36 (t, J = 7.8 Hz, 1H), 7.42 (t, J = 7.5 Hz, 2H), 7.48 (d, J = 7.3 Hz, 2H), 7.76 (d, J = 8.7 Hz, 2H), 8.039 (s, 2H), 8.043 (dd, J_1 = 8.7 Hz, J_2 = 1.8 Hz, 1H), 8.20 (d, J = 1.7 Hz, 1H), 8.50 (d, J = 8.8 Hz, 1H); ^{13}C NMR (151 MHz, $CDCl_3$) δ 14.3, 22.8, 26.3, 26.3, 29.5, 29.55, 29.62, 29.78, 29.83, 29.86, 29.88, 29.91, 29.92, 30.57, 32.09, 32.10, 69.4, 70.4, 73.7, 107.3, 115.8, 124.9, 127.6, 128.3, 128.8, 129.1, 129.7, 129.9, 130.6, 131.5, 136.7, 141.6, 141.9, 145.5, 147.7, 153.7, 160.1; IR (KBr) v 2917, 2848, 1602, 1465, 1426, 1383, 1344, 1237, 1119 cm^{-1}; MALDI-MS, m/z 945 (100, $[M]^+$). Anal. Calcd for $C_{62}H_{91}N_3O_4$: C, 79.02; H, 9.73; N, 4.46. Found: C, 78.90; H, 9.90; N, 4.43.

1,6-bis(3,4,5-tridodecyloxyphenyl)-3-(4-(hydroxyl(phenyl)methyl)phenyl)-1,4-dihydrobenzo[*e*][1,2,4]triazin-4-yl (4[3])

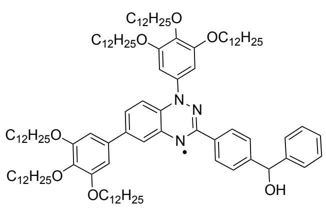 Compound **4[3]** was obtained by treatment of **2[3]** (1.0 g, 1.06 mmol) with excess 3,4,5-tridodecyloxyphenyllithium (2.63 equiv.) to give 970 mg (58% yield) of **5[3]** as a brown solid. R_f = 0.12 (SiO_2 pass, CH_2Cl_2/pet. ether 1:3). IR (KBr) v 2921, 2851, 1593, 1468, 1384, 1234, 1116 cm^{-1}; MALDI-MS, m/z 1574 (100, $[M]^+$). Anal. Calcd for $C_{104}H_{168}N_3O_7$: C, 79.44; H, 10.77; N, 2.67. Found: C, 79.50; H, 10.74; N, 2.71.

2. NMR spectra

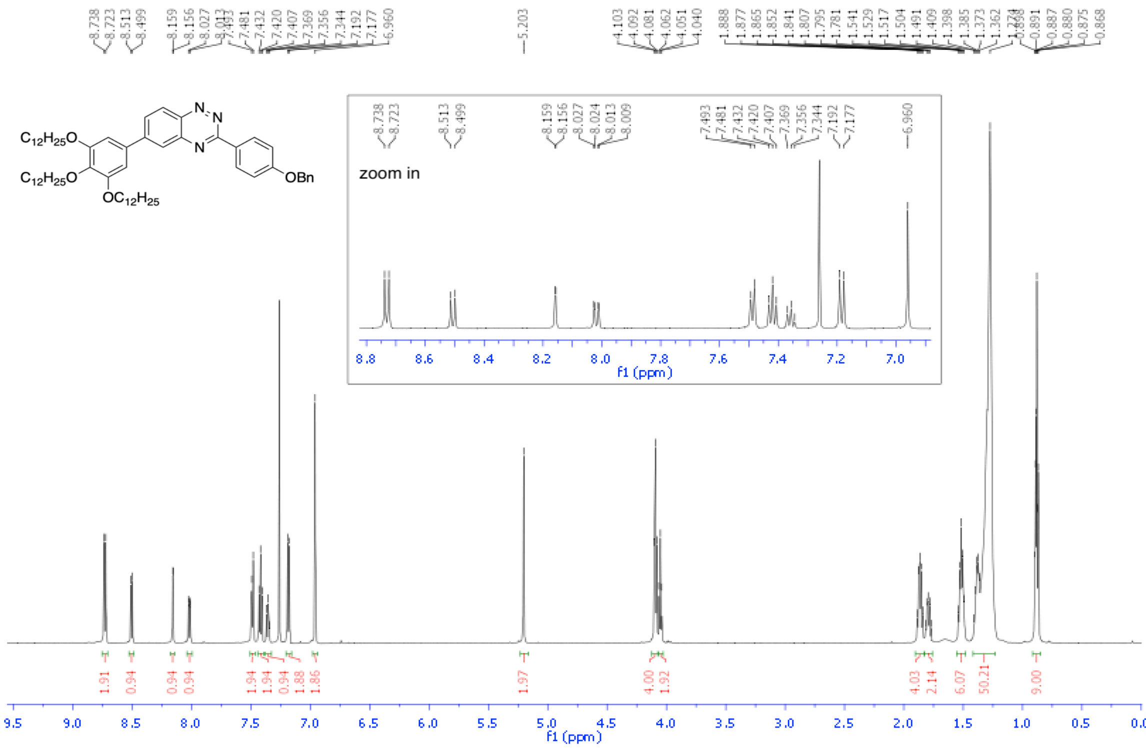

Figure S1. ^{1}H NMR of **2[3]** ($CDCl_3$, 600 MHz).

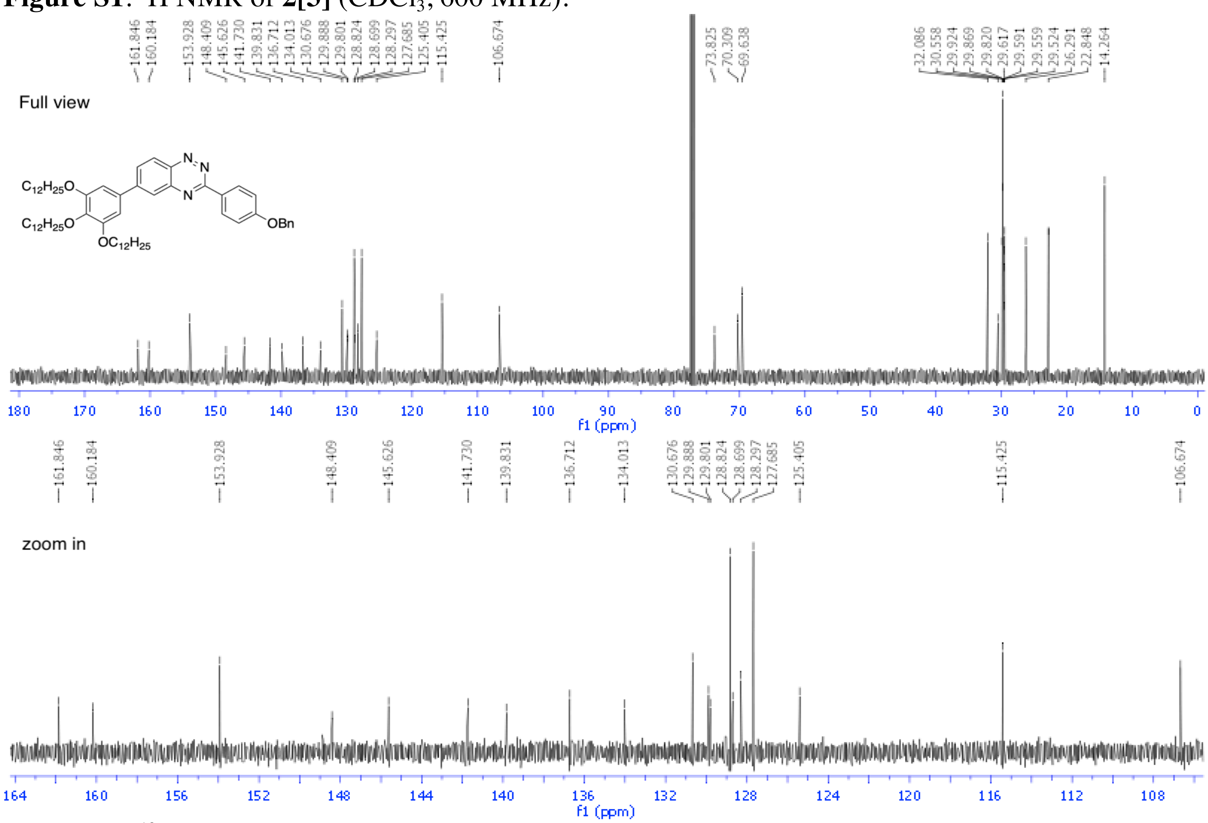

Figure S2. ^{13}C NMR of **2[3]** ($CDCl_3$, 151 MHz).

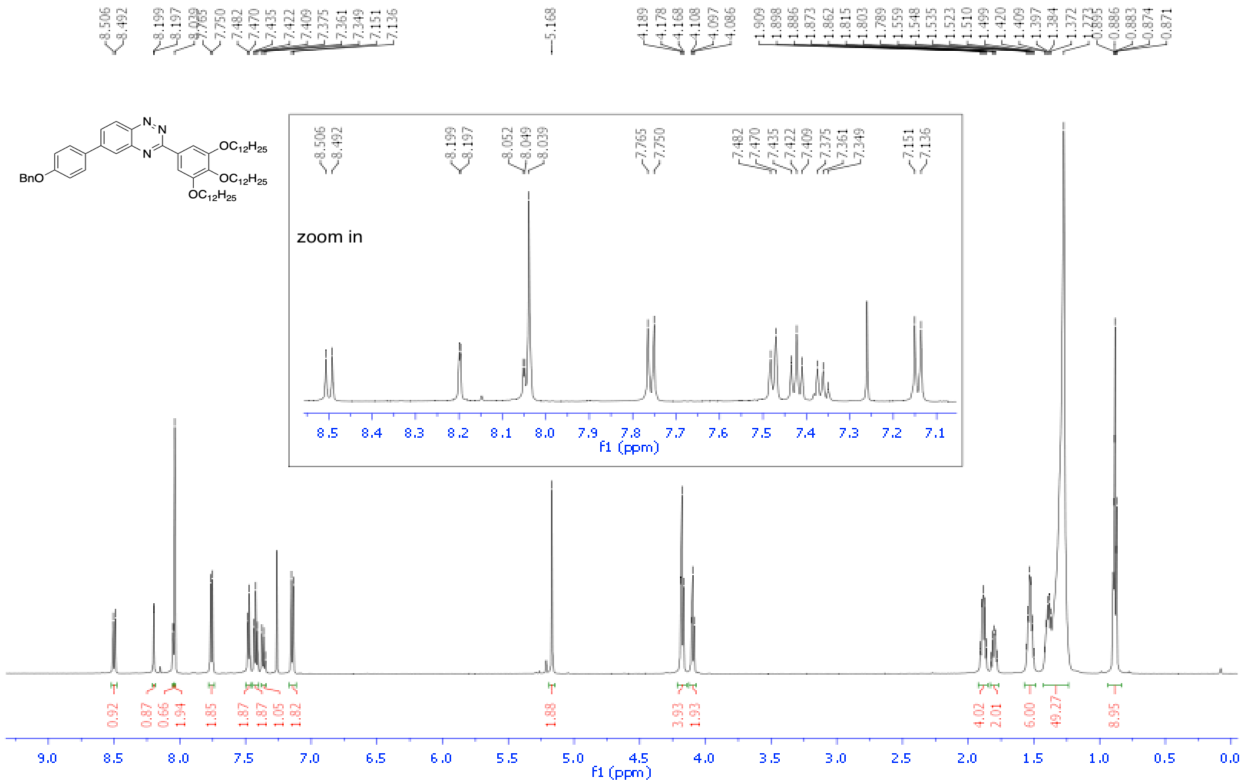

Figure S3. ^{1}H NMR for **2[6]** ($CDCl_3$, 600 MHz).

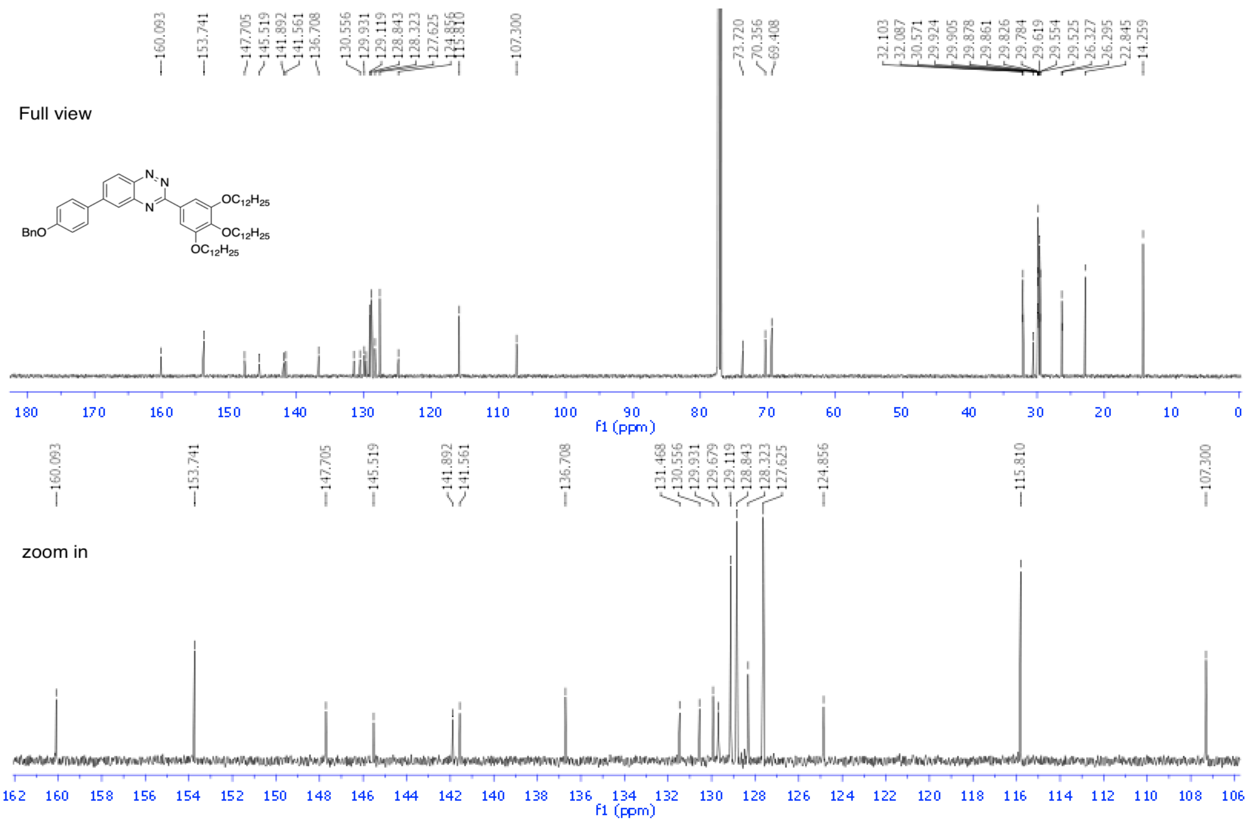

Figure S4. ^{13}C NMR for **2[6]** ($CDCl_3$, 151 MHz).

3. Thermal analysis

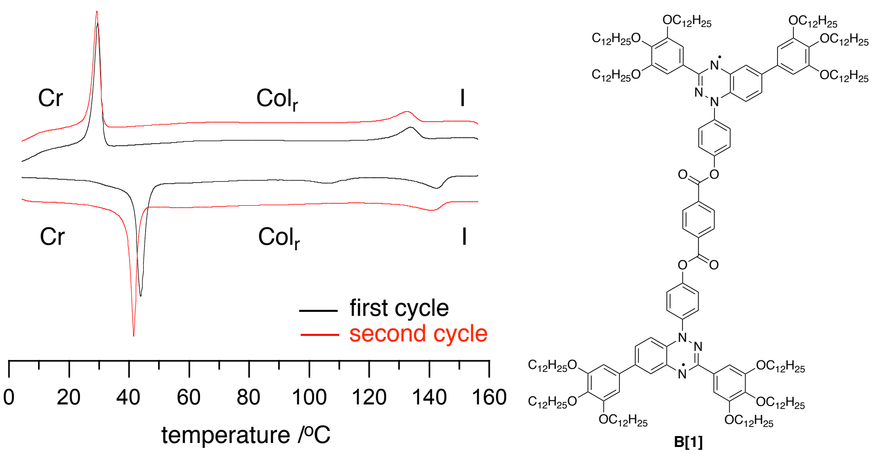

Figure S5. DSC traces of **B[1]**. Heating and cooling rates are 5 Kmin^{-1}.

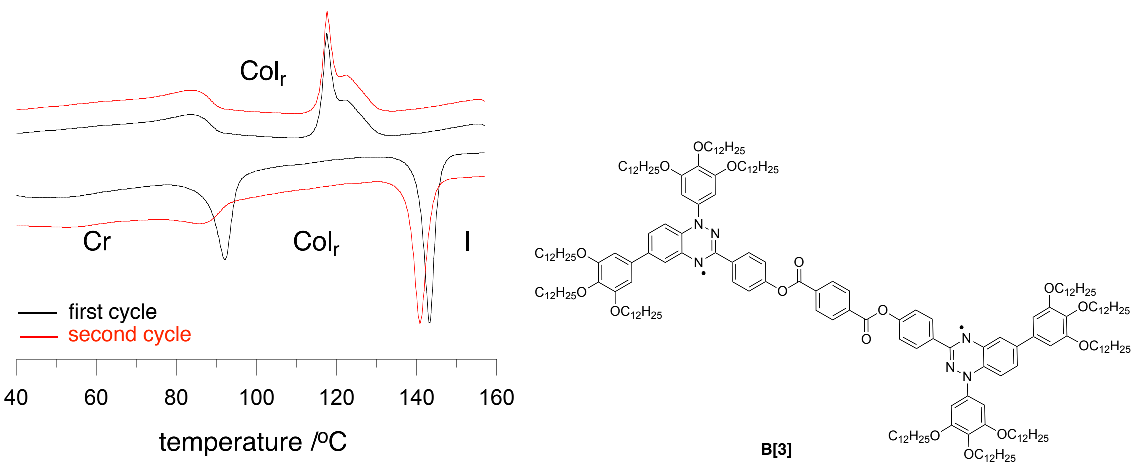

Figure S6. DSC traces of **B[3]**. Heating and cooling rates are 5 Kmin^{-1}.

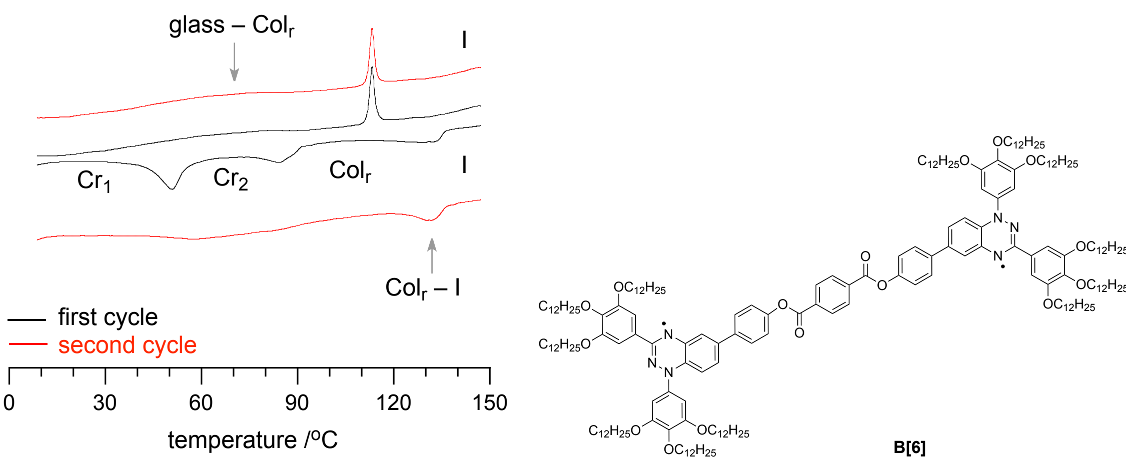

Figure S7. DSC traces of **B[6]**. Heating and cooling rates are 5 Kmin^{-1}.

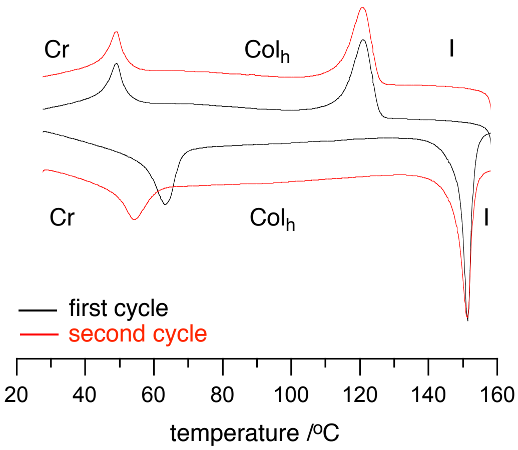

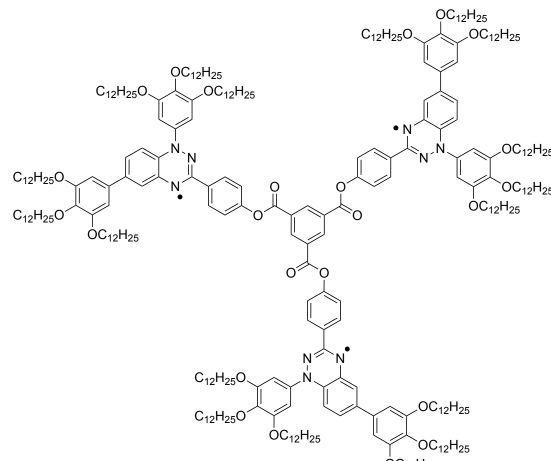

T[3]

Figure S8. DSC traces of **T[3]**. Heating and cooling rates are 5 Kmin^{-1}.

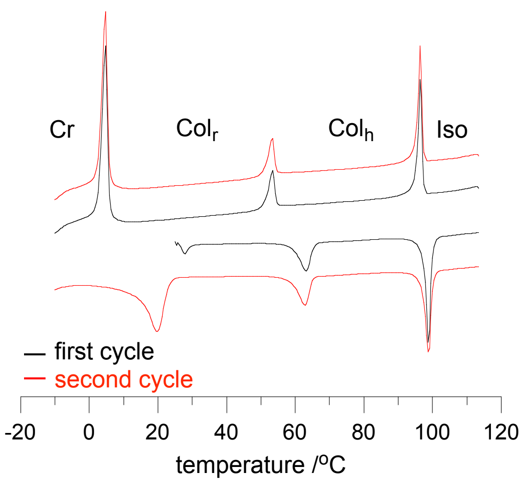

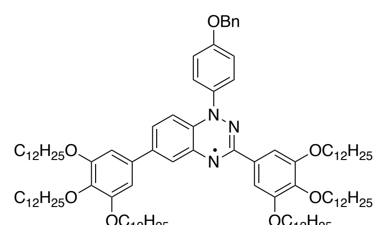

3[1]

Figure S9. DSC traces of **3[1]**. Heating and cooling rates are 5 Kmin^{-1}.

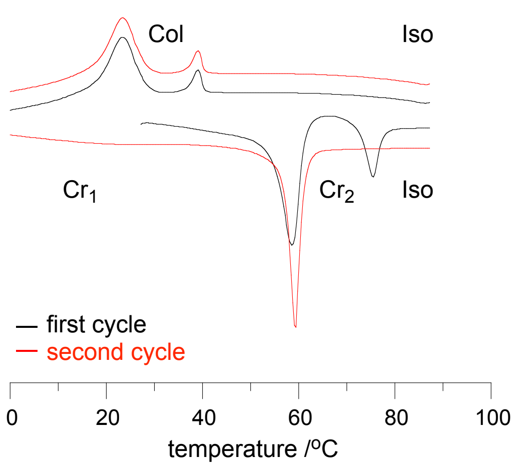

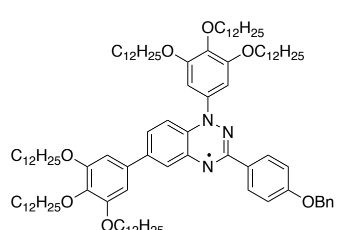

3[3]

Figure S10. DSC traces of **3[3]**. Heating and cooling rates are 5 Kmin^{-1}.

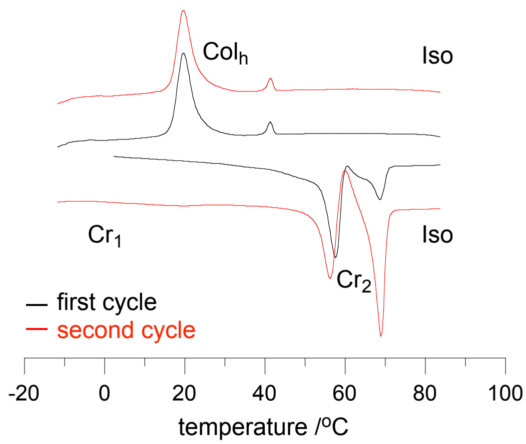

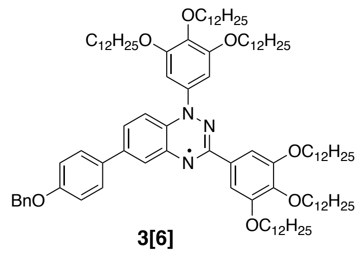

3[6]

Figure S11. DSC traces of **3[6]**. Heating and cooling rates are 5 $Kmin^{-1}$.

4. Powder XRD data

X-ray diffraction experiments were conducted with Bruker D8 GADDS system, equipped with ceramic tube with Copper anode, parabolic Göbel mirror monochromator, 0.5 mm point collimator and area detector Vantec 2000. Non-aligned (powder-like) samples were prepared in a form of a droplet on a heated surface and thermostated with a modified Linkam heating stage. Recorded two-dimensional diffraction patterns were integrated over azimuthal angle to obtain dependence of diffracted intensity on the diffraction angle 2θ. Results were analyzed with Bruker Topas software, which allowed simulation of patterns for chosen lattice symmetry with unit cell parameters treated as fitted variables.

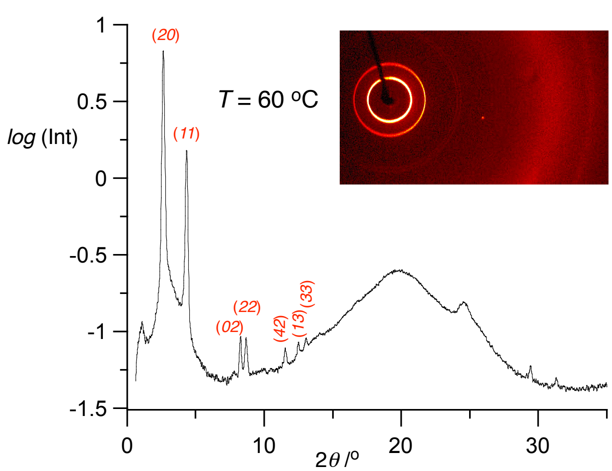

d_{exp} /Å	(hk)	d_{calc} /Å
33.5	(20)	33.5
20.4	(11)	20.4
10.7	(02)	10.7
10.2	(22)	10.2
7.7	(42)	7.7
7.1	(13)	7.1
6. 8	(33)	6.8

Figure S12. Left: X-ray diffractogram for **B[1]** obtained by integration of the 2D patterns at 60 °C (inset): Col_r, a = 66.9 Å, b = 21.4 Å, diffused 4.46 Å and 3.62 Å. Two weak signals at diffraction angle close to 30 deg. are artifacts, due to the sample holder. Right: experimental and calculated d spacing and Miller indexing.

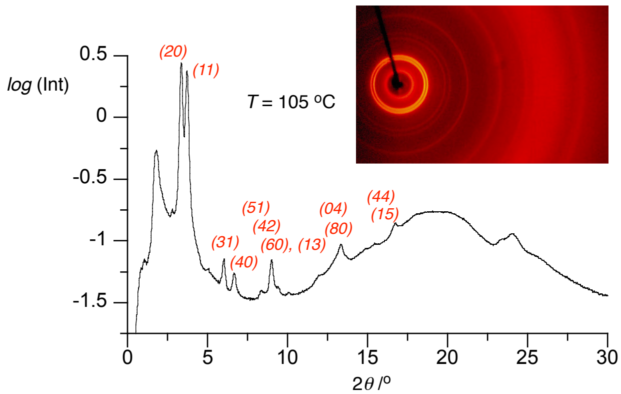

d_{exp} /Å	(*hk*)	d_{calc} /Å
26.4	(20)	26.4
23.8	(11)	23.8
14.7	(31)	14.7
13.3	(02)	13.4
	(40)	13.2
9.8	(51)	9.8
9.4	(42)	9.4
6.7	(04)	6.7
5.3	(15), (64)	5.3

Figure S13. Left: X-ray diffractogram for **B[3]** obtained by integration of the 2D patterns at 105 °C (inset): *Col*$_r$, a = 52.8 Å, b = 26.7 Å, diffused 4.60 Å and 3.70 Å. Right: experimental and calculated *d* spacing and Miller indexing.

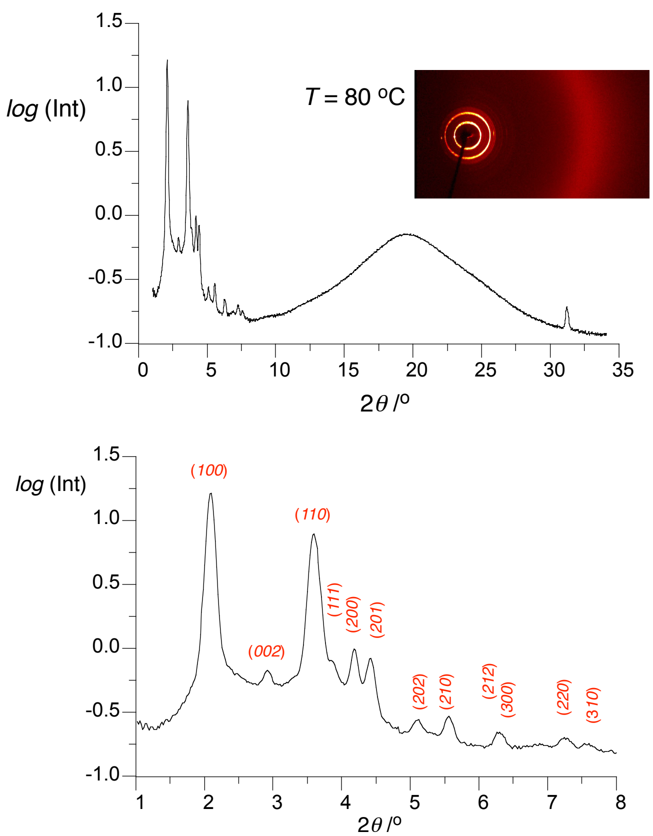

d_{exp} /Å	(*hkl*)	d_{calc} /Å
42.3	(100)	42.3
30.3	(002)	30.4
24.6	(102)	24.7
	(110)	24.4
22.9	(111)	22.6
21.1	(200)	21.1
20.0	(201)	20.0
17.2	(202)	17.3
15.9	(210)	16.0
14.0	(212)	14.1
	(003)	14.1
12.2	(220)	12.2
11.6	(310)	11.7

Figure S14. Left: X-ray diffractogram for **B[6]** obtained by integration of the 2D patterns at 80 °C (inset): *Col*$_{h(3D)}$, a = 48.8 Å, c = 60.7 Å, diffused 4.5 Å and 3.6 Å. The weak signal at the diffraction angle close to 32 deg. is an artifact due to the sample holder. Right: experimental and calculated *d* spacing and Miller indexing.

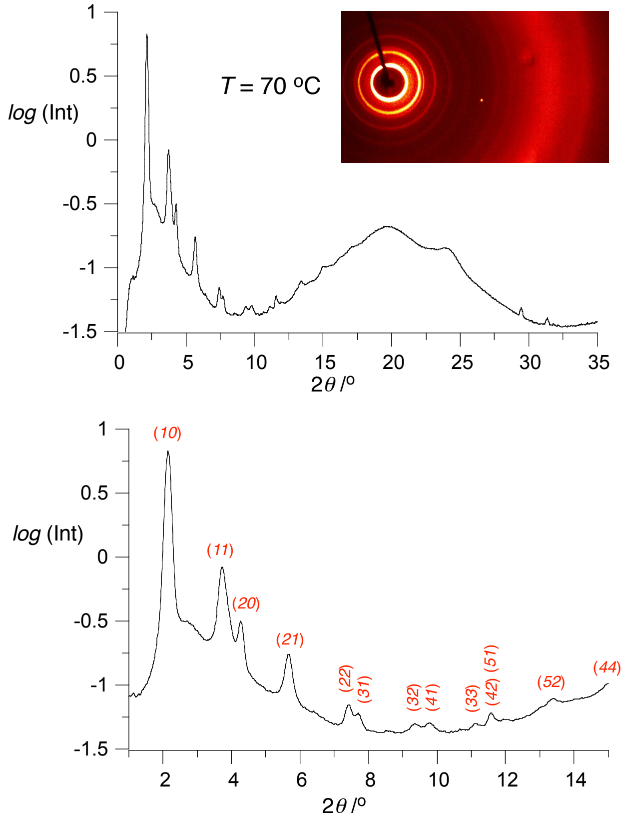

d_{exp} /Å	(*hk*)	d_{calc} /Å
41.2	(10)	41.2
23.6	(11)	23.7
20.7	(20)	20.6
15.6	(21)	15.6
11.9	(22)	11.9
11.4	(31)	11.4
9.5	(32)	9.4
9.0	(41)	9.0
8.0	(33)	7.9
7.6	(42)	7.8
	(51)	7.4
6.6	(52)	6.6
5.9	(44)	5.9

Figure S15. Left: X-ray diffractogram for **T[3]** obtained by integration of the 2D patterns at 70 ºC (inset): *Col*$_h$, *a* = 47.5 Å, diffused 4.52 Å and 3.69 Å. Two weak signals at diffraction angle close to 30 deg. are artifacts due to the sample holder. Right: experimental and calculated *d* spacing and Miller indexing.

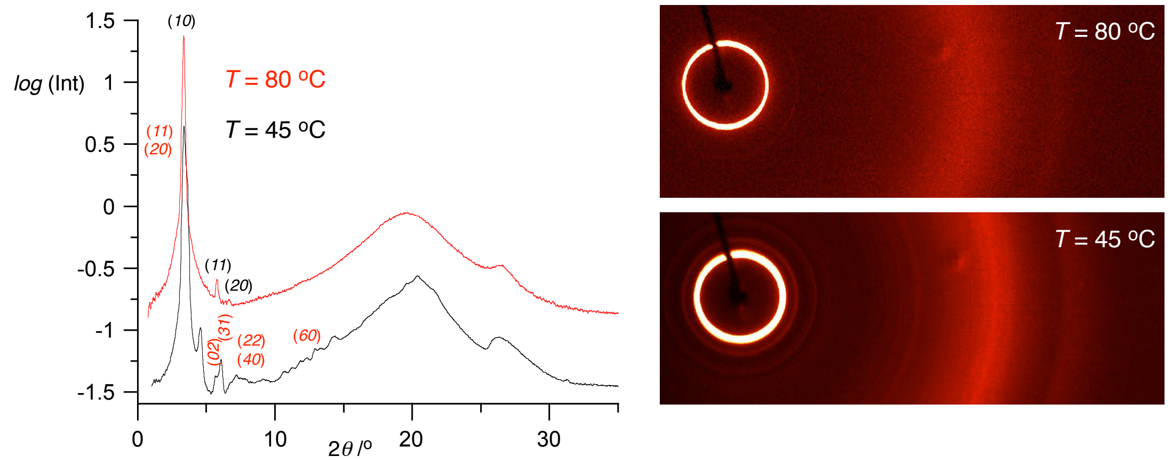

T	d_{exp} /Å	(*hk*)	d_{calc} /Å	T	d_{exp} /Å	(*hk*)	d_{calc} /Å
80 °C	26.4	(10)	26.4	80 °C	26.2	(11)	26.2
	15.3	(11)	15.2		24.6	(20)	24.6
	13.3	(20)	13.2		19.4		
					15.4	(02)	15.5
					14.6	(31)	14.5
					12.4	(22) (40)	12.4
					8.2	(60)	8.2
					7.8	(04)	7.8

Figure S16. Top: X-ray diffractogram for **3[1]** obtained by integration of the 2D patterns for both columnar phases: for *Col*$_r$ at 45 ^{o}C (black line, red labels), a = 49.2 Å, b = 31.0 Å, and for *Col*$_h$ at 80 ^{o}C (red line, black labels), a = 30.5 Å. Bottom: experimental and calculated d spacing and Miller indexing.

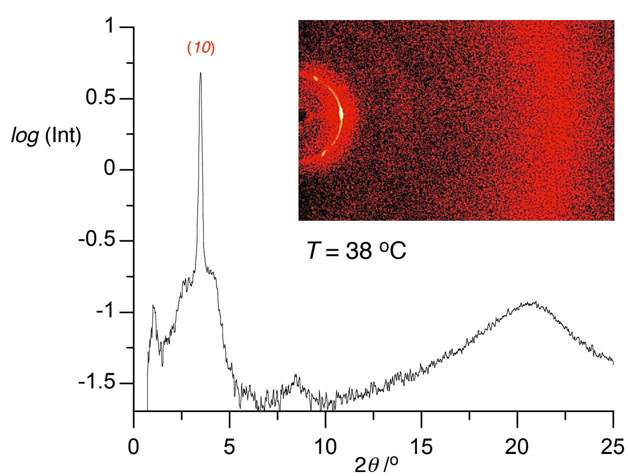

d_{exp}	(hk)	d_{calc}
25.3	(10)	25.3

Figure S17. Left: X-ray diffractogram for **3[6]** obtained by integration of the 2D patterns at 38 ^{o}C (inset): *Col*$_h$, a = 29.2. Right: experimental and calculated d spacing and Miller indexing.

5. Magnetization measurements and data analysis

5.1. SQUID

General procedure

A microcrystalline sample of the radical was placed in a polycarbonate capsule fitted in a plastic straw and its magnetization M was measured using a SQUID magnetometer (Quantum Design MPMS-XL-7T) as a function of applied field B (0–7 T) and as function of temperature T (rate of 1 K min^{-1}) in the following order: a) $M(B)$ at 2, 5, 7, 10, 15, 20, 300 K, b) $M(T)$ on cooling (300 K→ 2 K) at 6000 Oe. The only exception is the sample of monoradical **M[1]**, for which earlier data[3] obtained in the temperature range 2–400–2 K at 1000 Oe was analyzed as described below.

To avoid discontinuity in $M(T)$ plots due to magnetization crossing through zero, raw electrical signals were processed as follows.

For a given temperature T magnetization M was measured. Raw data collected by SQUID magnetometer at each such a point are electric signals $U(x)$ measured as a function of sample position x in the SQUID pick-up coil (so called second-order gradiometer, Figure S18). To avoid crossing through zero, the $U(x)$ function is modified with a function $U_{add}(x)$ to obtain a modified function $U_{mod}(x) = U(x) - U_{add}(x)$. The $U_{add}(x)$ function was derived from the original $U(x)$ function at 300 K and multiplied by a factor of 10. In addition, the position of the $U_{add}(x)$ function is shifted to overlap with the extrema in the original $U(x)$ function obtained at low temperatures. The temperature for the original function $U(x)$ (300 K) and the multiplication factor (10) for obtaining $U_{add}(x)$ function were selected arbitrally. Such a modification of each raw datapoint ($U(x)$ function for each temperature) is equivalent to adding a precisely known amount of "positive diamagnetism" to the sample. The resulting difference of signals, $U_{mod}(x) = U(x) - U_{add}(x)$, was fitted to an analytical function provided by Quantum Design MPMS (Application Note 1014-213 https://www.qdusa.com/sitedocs/appNotes/mpms/1014-213.pdf), which gave a magnetic moment value M_{mod} containing the added "positive diamagnetism". To obtain the actual magnetisation M of the sample, the resulting value M_{mod} is diminished by magnetization M_{add}, which precisely corresponds to the value derived from function $U_{add}(x)$. This procedure was applied for each experimental data point to obtain $M(T)$ and $M(B)$ values and executed using an algorithm written in MatLab program (version R2019a). The corrected data of magnetization of the sample was used for further analysis.

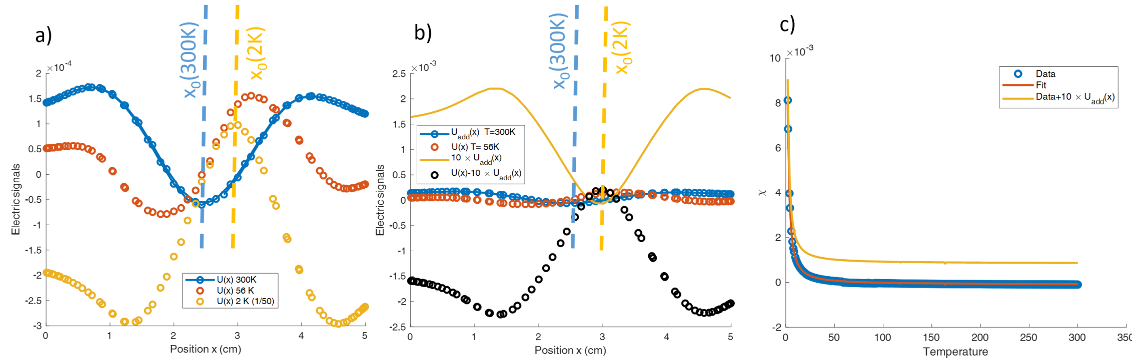

Figure S18. Examples of raw data analysis: a) electrical signals *U(x)* collected at 2 K (yellow, divided by 50), at 56 K (red) and at 300 K (blue); vertical dashed lines mark minimum of high temperature signal (blue) and maximum of low temperature signal (yellow); *b)* symmetric paramagnetic-type signal (black) obtained from the original asymmetric signal *U(x)* (red) by addition of $U_{add}(x)$ (yellow) *c)* conversion of M_{mod} (yellow) by subtracting M_{add} to obtain original magnetization *M* (blue).

Analysis of magnetization data obtained for all samples as described above was performed by calculating molar total magnetic susceptibility, χ, and subsequently establishing diamagnetic correction, χ_{dia}, to calculate the paramagnetic component, χ_{p}, of the magnetic susceptibility. The diamagnetic correction (sample and the sample holder) was estimated from the linear portion of high temperature $\chi \bullet T$ *vs T* plot assuming ideal paramagnetic behavior of the sample and using the Curie law (eq 1).

$$\chi \bullet T = \left(\chi_p + \chi_{dia}\right) \bullet T = C + \chi_{dia} \bullet T \qquad \text{(eq 1)}$$

where $C = 0.375$ $\mathrm{cm^3mol^{-1}K}$ for an ideal paramagnet.

The mean-field interactions θ (the Weiss constant) was determined from a linear fit to the $1/\chi_{\mathrm{p}}(T)$ plots and using equation 2:

$$1/\chi_p = T \bullet 1/C - \theta/C \qquad \text{(eq 2)}$$

The exchange interaction energy in samples **M[6]**, **B[3]** and **T[3]** exhibiting ferromagnetic interactions was obtained by assuming a 1D ferromagnetic chain and fitting the low temperature $\chi_{\mathrm{p}}(T)$ data to the Baker's high temperature series expansion[4] (eq 3a and 3b)

$$\chi_p = \frac{N_A g^2 \mu_B^2}{4k_B T} \times \left[\frac{1+5.7979916x+16.902653x^2+29.376885x^3+29.832959x^4+14.036918x^5}{1+2.7979916x+7.008678x^2+8.6538644x^3+4.5743114x^4}\right]^{2/3} \qquad \text{(eq 3a)}$$

in which $x = \frac{J}{2k_B T}$

and after combining the constants:

$$\chi_p = \frac{C}{T} \times \left[\frac{1+5.797991x+16.902653x^2+29.376885x^3+29.832959x^4+14.036918x^5}{1+2.7979916x+7.008678x^2+8.6538644x^3+4.5743114x^4}\right]^{2/3} \quad \text{(eq 3b)}$$

For internal consistency, Curie constant C used for fitting with Baker's function (eq 3b) was taken form Curie-Weiss function fitting to eq 2. Values of parameter C used for fitting and the resulting exchange interaction energies J/k_B are listed in Table S1.

Analysis of the magnetic data for each experiment and compounds is complicated by mobility of the fluid phase in the capsule (geometry change) and partial sample realignment in the magnetic field due to a significant diamagnetic anisotropy. Results are presented in Figures S19–S139.

Table S1. Parameter C and exchange interaction energies for **M[n]**, **B[n]** and **T[n]**.

		$\chi_p \bullet T$ at 2K		Curie-Weiss analysis		Baker thermal expansion
compd	solid	cm^3 mol^{-1} K	C [a] /cm^3 mol^{-1}K	C [b] /cm^3 mol^{-1} K	θ /K	J/k_B [c] /K
M[1]	pristine	0.011	0.011	–	–	
	premelted	0.017	0.017	–	–	
M[3]	pristine	0.008	0.235	–		
	premelted	0.025	0.338	–		
M[6]	pristine	0.416	0.345	0.344	-0.3(1)	0.42(1)
	premelted	0.385	0.322	0.321	+1.1	0.40(1)
B[1]	pristine	0.061	0.156	–	–	
	premelted	0.073	0.068	–	–	
B[3]	pristine	1.000	0.379	0.362	+7.76	5.45
	premelted	0.538	0.283	0.278	+0.53	2.46
B[6]	pristine	0.116	0.253	0.284	-37.8	
	premelted	0.103	0.151	0.157	-10.5	
T[1]	pristine	0.113	0.191	0.202	-13.2	
	premelted	0.140	0.218	0.224	-6.7	
T[3]	pristine	0.657	0.322	0.314	+5.2	3.04
	premelted	0.458	0.272	0.261	+8.3	1.88
T[6]	pristine	0.110	0.253	0.334	-87	
	premelted	0.121	0.180	0.188	-11.4	

[a] Obtained from fitting to Curie law (eq. 1) to a high temperature portion of the $\chi \bullet T$ vs T plot. [b] Obtained from the fitting to Curie-Weiss law (eq. 2) to a low temperature portion of the $1/\chi_p$ *vs* T plot.
[c] Exchange interaction energy from fitting to the Baker's function (eq. 3b).

Monoradicals

M[1]. pristine solid. Raw data taken from an earlier report.[3]

m = 11.92 mg, 8.129×10^{-6} mol, M_w= 1466.34 g mol^{-1}

Total molar susceptibility, χ, of the sample as a function of temperature in the cooling mode is shown in Figure S19 and a χ•T *vs* T plot in Figure S20.

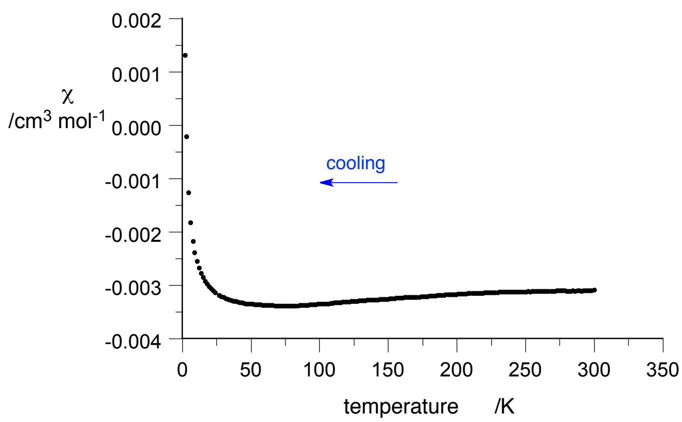

Figure S19. Molar magnetic susceptibility χ *vs* T obtained for pristine solid **M[1]** on cooling 300 K → 2 K at 0.1 T. The cooling rate is 0.8 K/min.

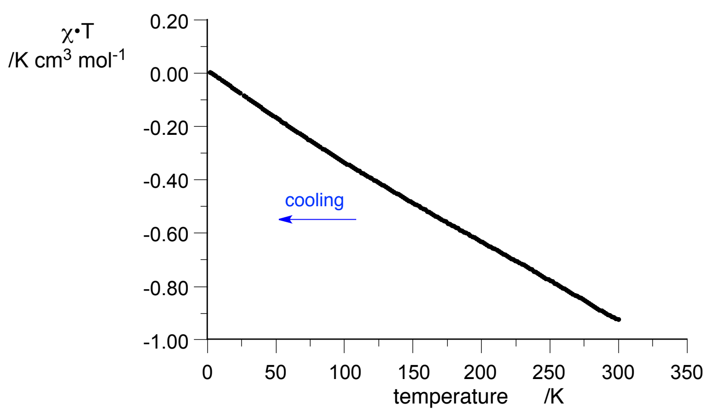

Figure S20. A χ•T *vs* T plot for pristine solid **M[1]** obtained on cooling 300 K → 2 K at 0.1 T. The cooling rate is 0.8 K/min.

The diamagnetic correction, χ_{dia}, was determined from a linear portion of the χ•T *vs* T plot (Figure S20) in the temperature range 50 K – 2 K (Figure S21).

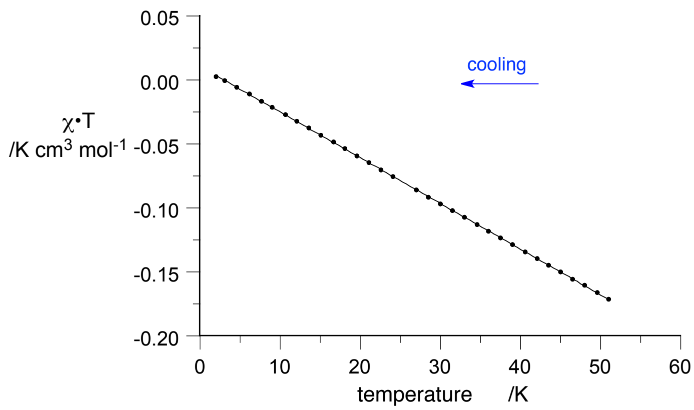

Figure S21. A linear portion of the χ•T *vs* T plot for pristine solid **M[1]** (Figure S20) in the range of 50 K –2 K. Best fit line: χ•T = -0.003567(3)•T + 0.0106(1), r^2 = 0.99998.

The diamagnetic correction of -0.003567•T $cm^3mol^{-1}K$ was applied to the χ•T plot and the resulting χ_p•T *vs* T plot is shown in Figure S22.

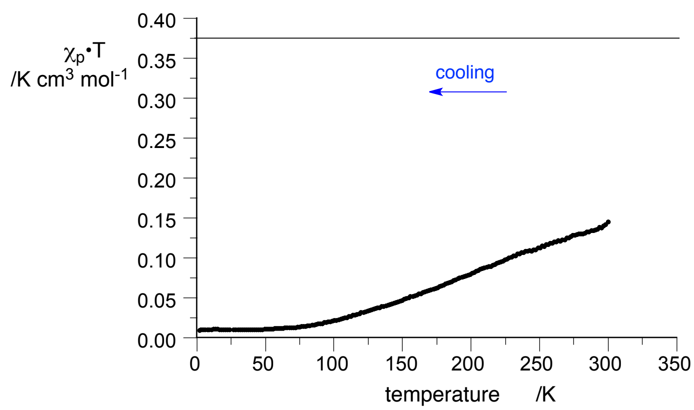

Figure S22. χ_p•T *vs* T plot for pristine solid **M[1]** in the cooling mode after diamagnetic correction, χ_{dia} = -0.003567 cm^3mol^{-1}, determined in Figure S21. The horizontal line marks the value of 0.375 Kcm^3mol^{-1} for an ideal paramagnet.

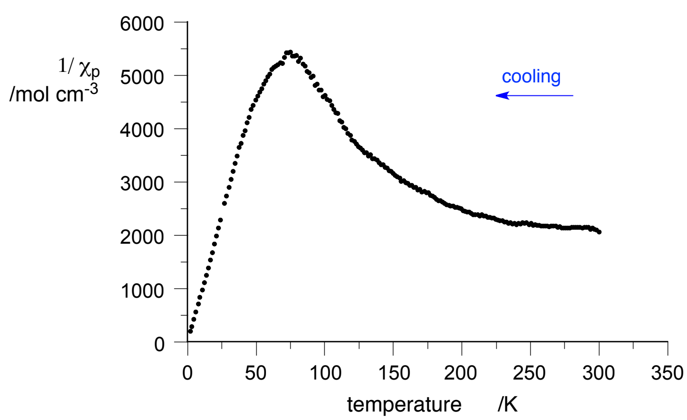

Figure S23. 1/χ_p *vs* T plot for pristine solid **M[1]** in the cooling mode.

The $1/\chi_p$ *vs* T plot for solid **M[1]** shown in Figure S23 is not linear which precludes the Curie-Weiss analysis.

M[1]. **Melted sample**. Raw data taken from an earlier report.[3]

The sample of **M[1]** in a polycarbonate capsule investigated above was heated to 400 K in the magnetometer, cooled down to 300 K and analyzed.

m = 11.92 mg, 8.129×10^{-6} mol, M_w= 1466.34 g mol^{-1}

Total molar susceptibility, χ, of the sample as a function of temperature in the cooling mode is shown in Figure S24 and a χ•T *vs* T plot in Figure S25.

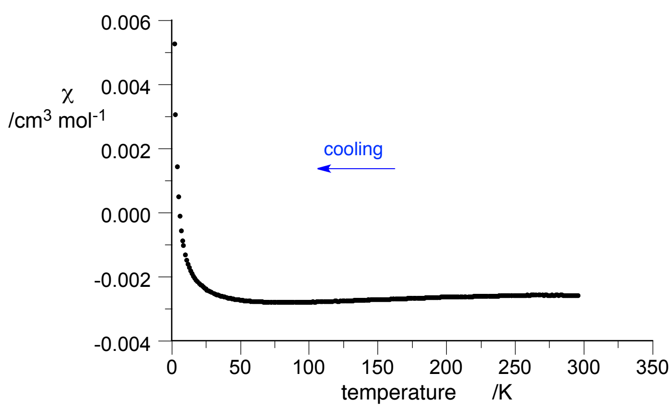

Figure S24. Molar magnetic susceptibility χ *vs* T obtained for melted **M[1]** on cooling 300 K → 2 K at 0.1 T. The cooling rate is 0.8 K/min.

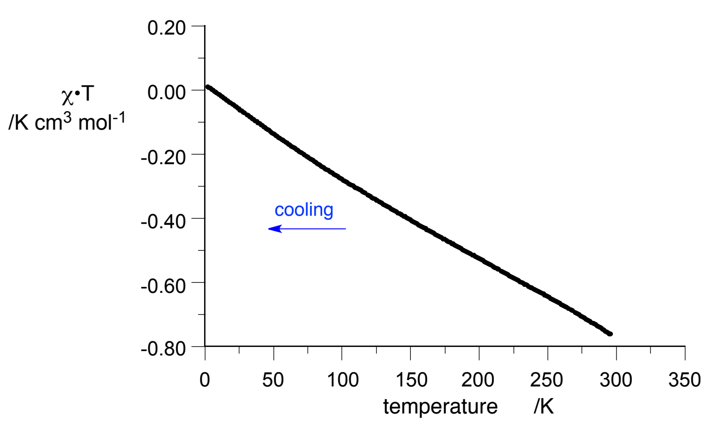

Figure S25. A χ•T *vs* T plot for melted **M[1]** obtained on cooling 300 K → 2 K at 0.1 T. The cooling rate is 0.8 K/min.

The diamagnetic correction, χ_{dia}, was determined from a linear portion of the χ•T *vs* T plot (Figure S25) in the temperature range 50 K – 2 K (Figure S26).

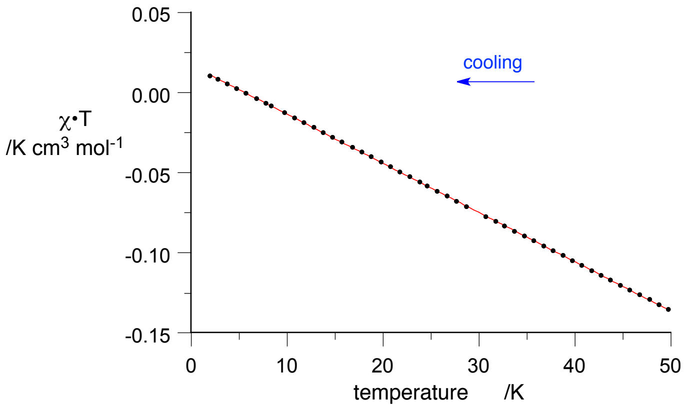

Figure S26. A linear portion of the χ•T *vs* T plot for melted **M[1]** (Figure S25) in the range of 50 K –2 K. Best fit line: χ•T = -0.003066(2)•T + 0.01712(5), r^2 = 0.99999.

The diamagnetic correction of -0.003066•T $cm^3mol^{-1}K$ was applied to the χ•T plot and the resulting χ_p•T *vs* T plot is shown in Figure S27.

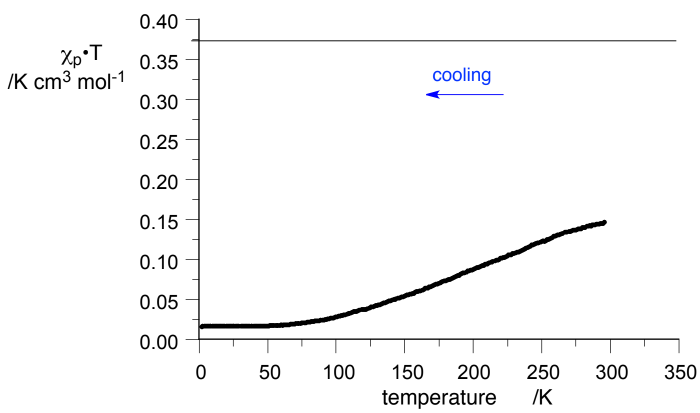

Figure S27. χ_p•T *vs* T plot for melted **M[1]** in the cooling mode after diamagnetic correction, χ_{dia} = -0.003066 cm^3mol^{-1}, determined in Figure S26. The horizontal line marks the value of 0.375 Kcm^3mol^{-1} for an ideal paramagnet.

The $1/\chi_p$ *vs* T plot for melted **M[1]** shown in Figure S28 is not linear which precludes the Curie-Weiss analysis.

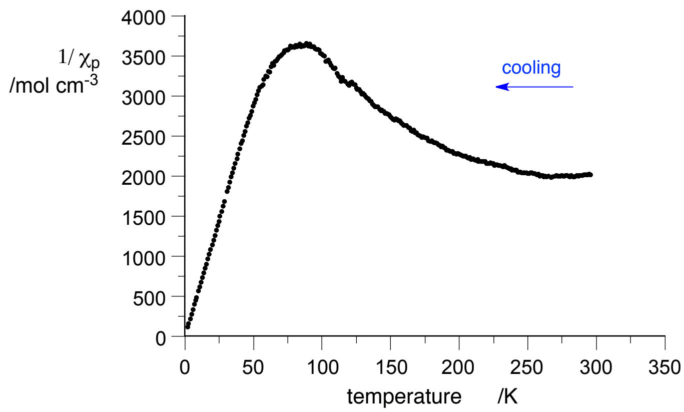

Figure S28. $1/\chi_p$ *vs* T plot for melted **M[1]** in the cooling mode.

A comparison of χ_p•T (T) plots for pristine and melted samples of **M[1]** are shown in Figures S29. Figure S30 shows a comparison of total molar magnetization in function of applied field B, $M_{tot}(B)$ at 2 K.

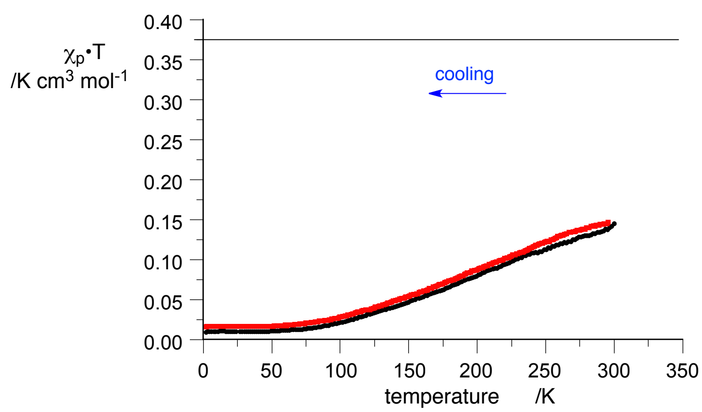

Figure S29. χ_p•T *vs* T plots for solid (black) and melted (red) sample of **M[1]** in the cooling mode. The horizontal line marks the value of 0.375 Kcm^3mol^{-1} for an ideal paramagnet.

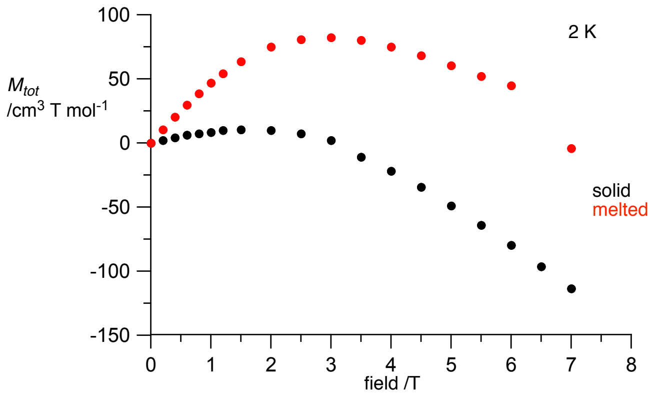

Figure S30. Molar total magnetization M_{mol} *vrs* field for solid (black) and melted (red) sample of **M[1]** at 2 K.

M[3]. pristine solid sample

m = 12.51 mg, 8.532×10^{-6} mol, M_w= 1466.34 g mol^{-1}

Total molar susceptibility, χ, of the sample as a function of temperature in the cooling mode is shown in Figure S31 and a χ•T *vs* T plot in Figure S32.

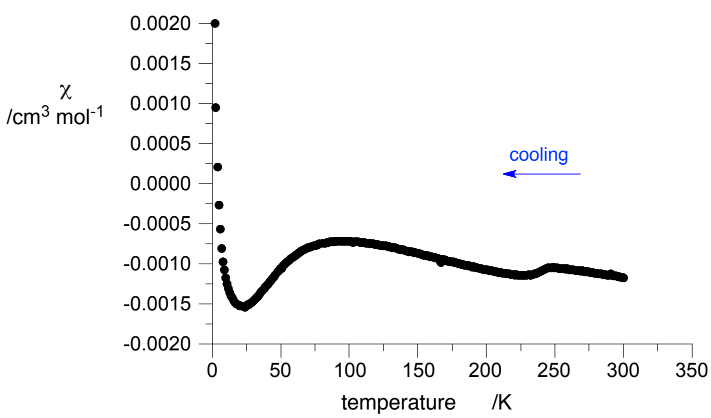

Figure S31. Molar magnetic susceptibility χ *vs* T obtained for solid **M[3]** in the cooling mode 300 K → 2 K at 0.6 T. The cooling rate is 1 K/min.

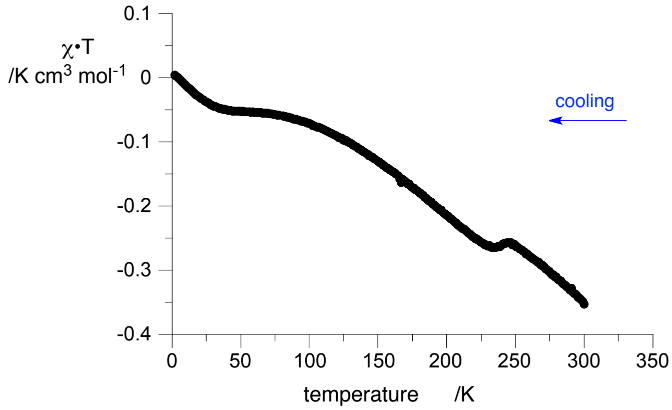

Figure S32. A χ•T *vs* T plot for solid **M[3]** obtained in the cooling cycle 300 K → 2 K at 0.6 T. The cooling rate is 1 K/min.

The diamagnetic correction, χ_{dia}, was determined from a linear portion of the χ•T *vs* T plot (Figure S32) in the temperature range 280 K – 300 K (Figures S33).

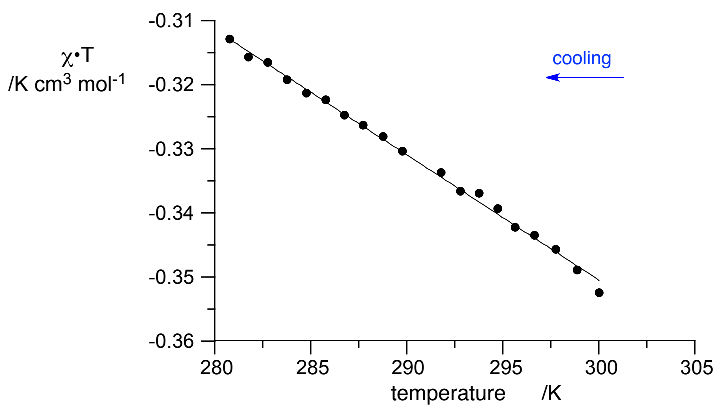

Figure S33. A linear portion of the χ•T *vs* T plot for solid **M[3]** (Figure S32) in the range of 280 K → 300 K. Best fit line: χ•T = -0.001951(30)•T + 0.235(8), r^2 = 0.996.

The diamagnetic correction of -0.001951•T $cm^3mol^{-1}K$ was applied to the χ•T plot in the cooling mode and the resulting χ_p•T *vs* T plot is shown in Figure S34, while the $1/\chi_p$ *vs* T plot for solid **M[3]** shown in Figure S35.

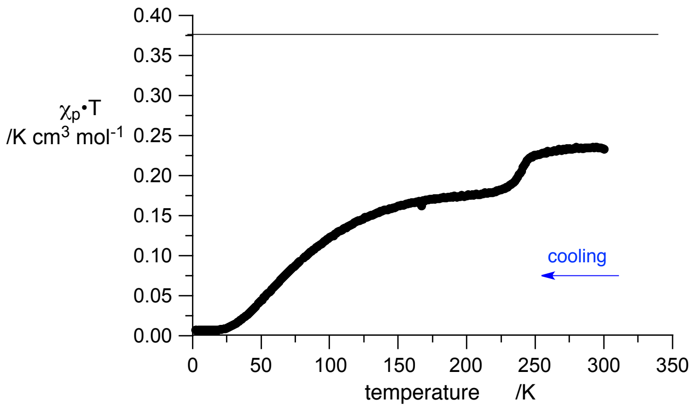

Figure S34. χ_p•T *vs* T plot for solid **M[3]** in the cooling mode after diamagnetic correction, , χ_{dia} = -0.001951 cm^3mol^{-1}, determined in Figure S32. The horizontal line marks the value of 0.375 Kcm^3mol^{-1} for an ideal paramagnet.

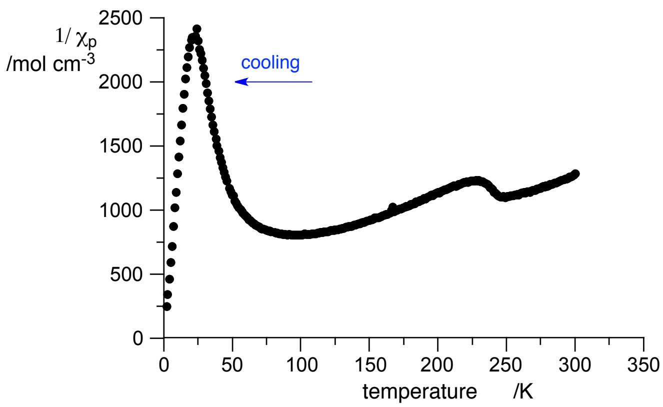

Figure S35. 1/χ_p *vs* T plot for solid **M[3]** in the cooling mode.

The non-linear 1/χ_p *vs* T plot precludes the Curie-Weiss analysis.

Figure S36 shows total molar magnetization in function of applied field B, $M_{tot}(B)$ at selected temperatures.

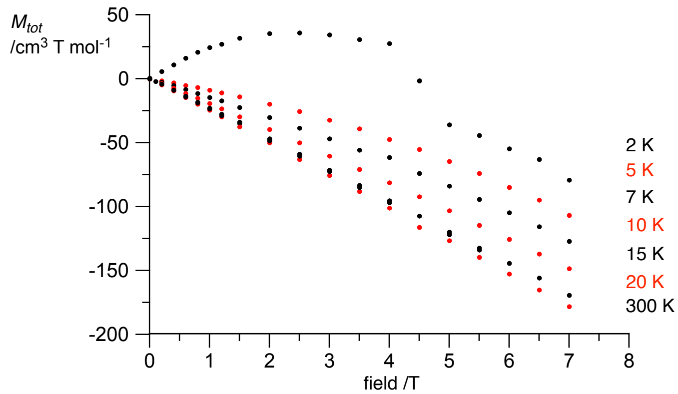

Figure S36. Molar total magnetization M_{mol} *vs* field for solid **M[3]** at selected temperatures.

M[3]. melted sample

m = 12.51 mg, 8.532×10^{-6} mol, M_w= 1466.34 g mol^{-1}

Sample of **M[3]** in a polycarbonate capsule investigated above was briefly heated to 400 K in the magnetometer, cooled down to 300 K and analyzed.

Total molar susceptibility, χ, of the sample as a function of temperature in the cooling mode is shown in Figure S37 and a χ•T *vs* T plot in Figure S38.

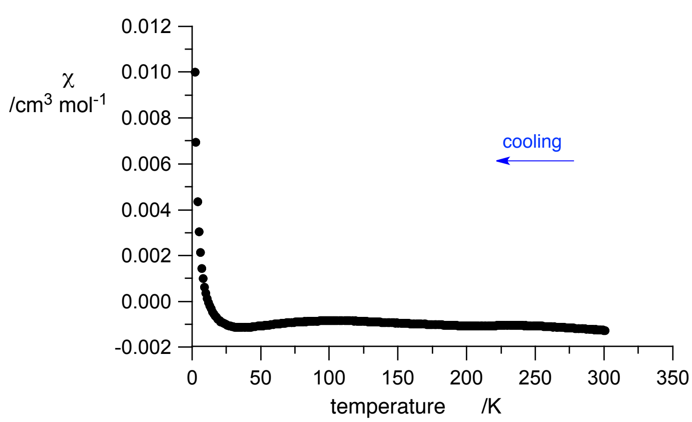

Figure S37. Molar magnetic susceptibility χ *vs* T obtained for melted **M[3]** in the cooling mode 300 K → 2 K at 0.6 T. The heating rate is 1 K/min.

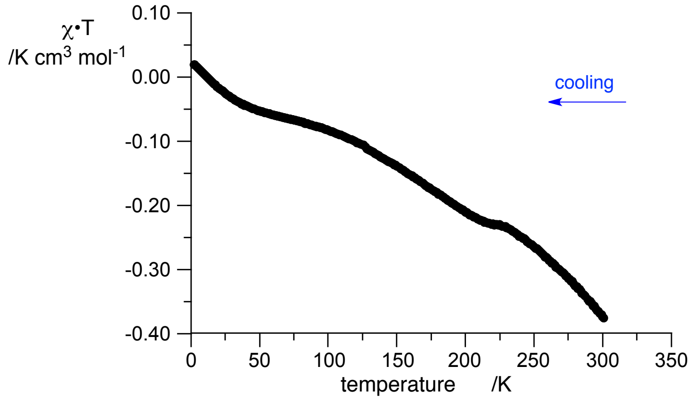

Figure S38. A χ•T *vs* T plot for melted **M[3]** obtained on cooling mode 300 K → 2 K at 0.6 T. The cooling rate is 1 K/min.

The diamagnetic correction, χ_{dia}, was determined from a linear portion of the χ•T *vs* T plot (Figure S38) in the temperature range 300 K – 270 K (Figure S39).

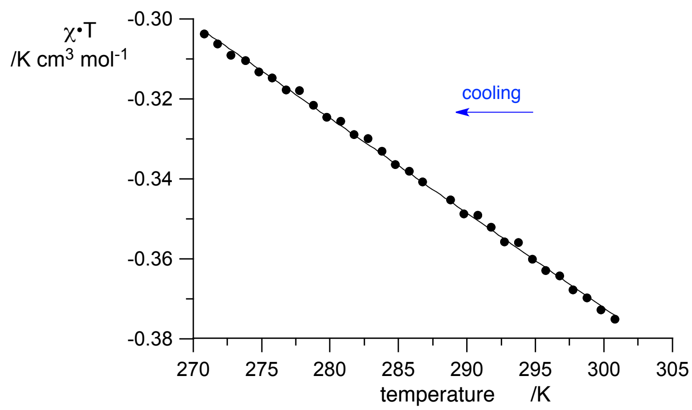

Figure S39. A linear portion of the χ•T *vs* T plot for melted **M[3]** (Figure S38) in a range of 270 K → 300 K. Best fit line: χ•T = -0.002367(18)•T + 0.338(5), r^2 = 0.998.

The diamagnetic correction of -0.002367•T $cm^3mol^{-1}K$ was applied to the χ•T plot and the resulting χ_p•T *vs* T plot is shown in Figure S40.

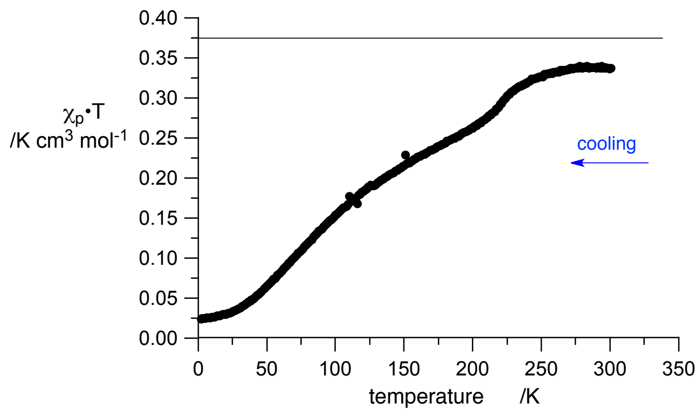

Figure S40. χ_p•T plot *vs* T for melted **M[3]** in the cooling mode after diamagnetic correction χ_{dia} = -0.002367 cm^3mol^{-1} determined in Figure S39. The horizontal line marks the value of 0.375 Kcm^3mol^{-1} for an ideal paramagnet.

The $1/\chi_p$ *vs* T plot for melted **M[3]** shown in Figure S41 is non-linear, which precludes the Curie-Weiss analysis.

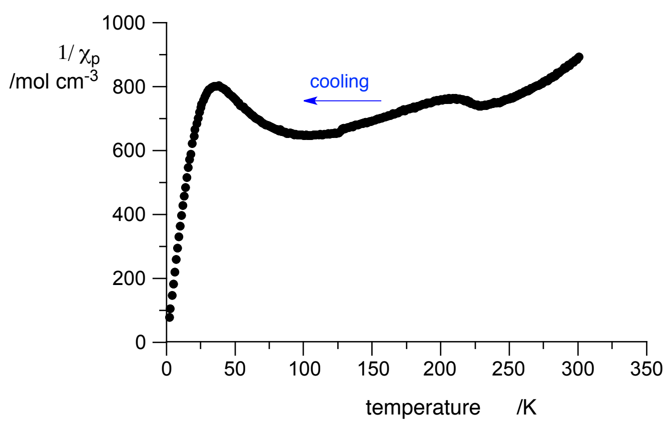

Figure S41. $1/\chi_p$ *vs* T plot for melted **M[3]** in the cooling mode.

Figure S42 shows total molar magnetization in function of applied field B, $M_{tot}(B)$ at selected temperatures.

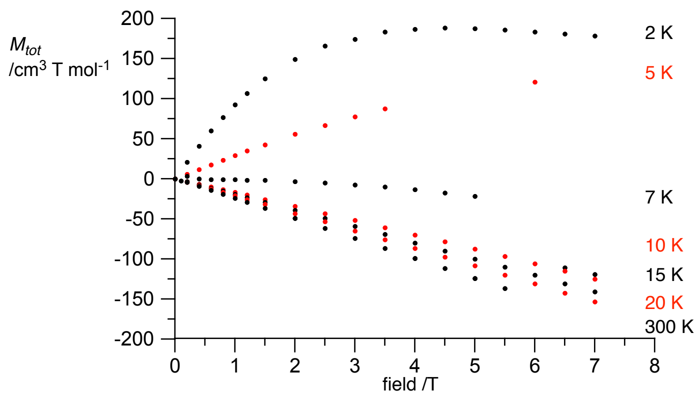

Figure S42. Molar total magnetization M_{mol} *vrs* field for melted **M[3]** at selected temperatures.

A comparison of χ_p•T (T) plots for pristine and melted samples of **M[3]** is shown in Figure S43.

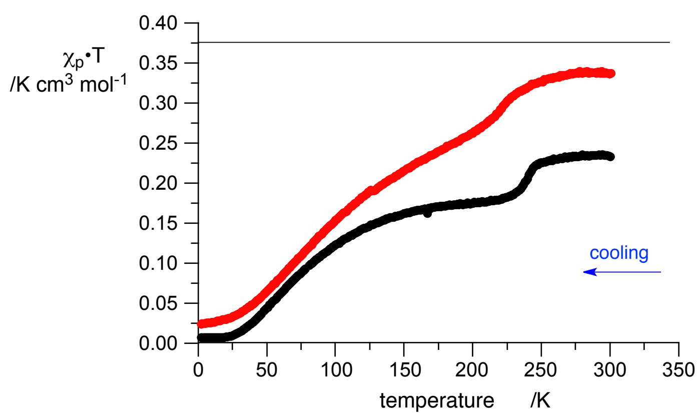

Figure S43. χ_p•T *vs* T plots for solid (black) and melted (red) sample of **M[3]** in the cooling mode. The horizontal line marks the value of 0.375 Kcm^{3}mol^{-1} for an ideal paramagnet.

Monoradical **M[6]**. **pristine solid sample**

m = 16.42 mg, 11.198×10^{-6} mol, M_w= 1466.34 g mol^{-1}

Total molar susceptibility, χ, of the sample as a function of temperature in the cooling mode is shown in Figure S44 and the χ•T *vs* T plot in Figure S45.

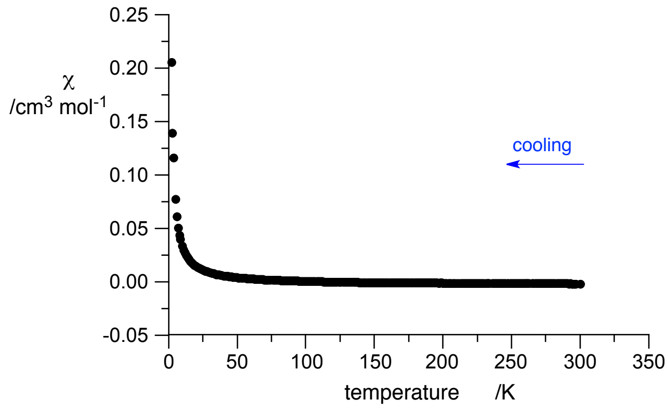

Figure S44. Molar magnetic susceptibility χ *vs* T obtained for pristine sample of **M[6]** on cooling 300 K → 2 K at 0.6 T. The cooling rate is 1 K/min.

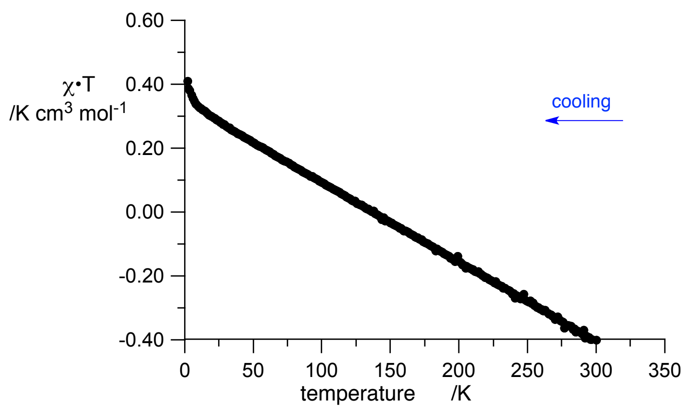

Figure S45. A χ•T *vs* T plot for solid **M[6]** obtained on cooling 300 K → 2 K at 0.6 T. The cooling rate is 1 K/min.

The diamagnetic correction, χ_{dia}, was determined from a linear portion of the χ•T *vs* T plot (Figure S45) in the temperature range 300 K – 200 K (Figure S46).

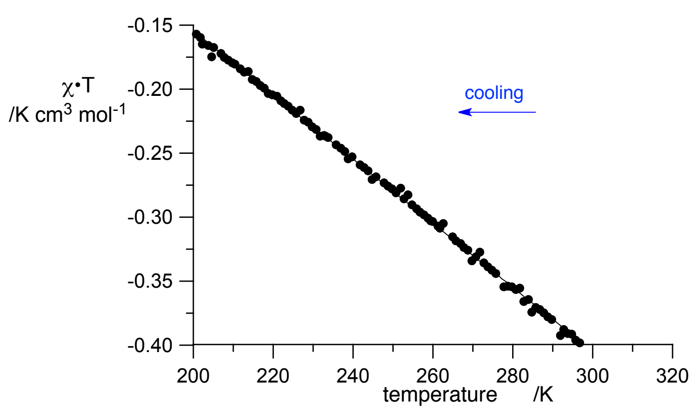

Figure S46. A linear portion of the χ•T *vs* T plot for solid **M[6]** (Figure S45) in the range of 200 K → 300 K. Best fit line: χ•T = -0.002500(9)•T + 0.345(2), r^2 = 0.999.

The diamagnetic correction of -0.002500•T $cm^3mol^{-1}K$ was applied to the χ•T plot in and the resulting χ_p•T *vs* T plot is shown in Figure S47.

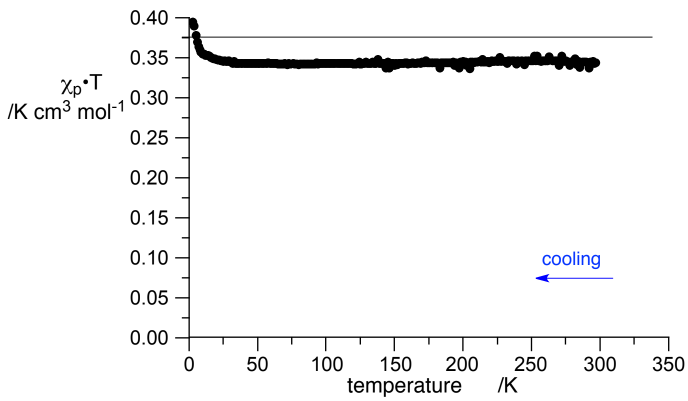

Figure S47. χ_p•T *vs* T plot for solid **M[6]** in the cooling mode after diamagnetic correction , χ_{dia} = -0.002500 cm^3mol^{-1} determined in Figures S46. The horizontal line marks the value of 0.375 Kcm^3mol^{-1} for an ideal paramagnet.

Analysis of the 1/χ_p *vs* T plot in Figure S48 according equation 2 gives the value C = 0.344 $cm^3mol^{-1}K$ and the Weiss constant θ = -0.3(1) K.

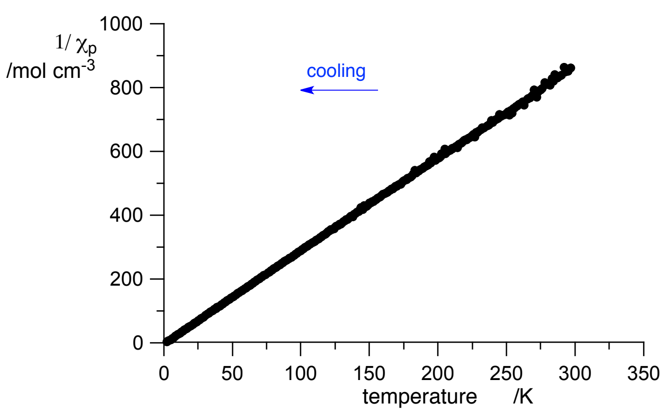

Figure S48. 1/χ_p *vs* T plot for solid **M[6]** in the cooling mode. Best fit function in the range 50–200 K: 1/χ_p = 0.78(45)+2.908(3)•T, r^2 = 0.9998.

The $\chi_p(T)$ plot (Figure S47) in the temperature range of 2–200 K was fitted to Baker's function (eq. 3b) using Curie constant C established in Figure S47 (C = 0.344 $cm^3mol^{-1}K$) and the result is shown in Figure S49.

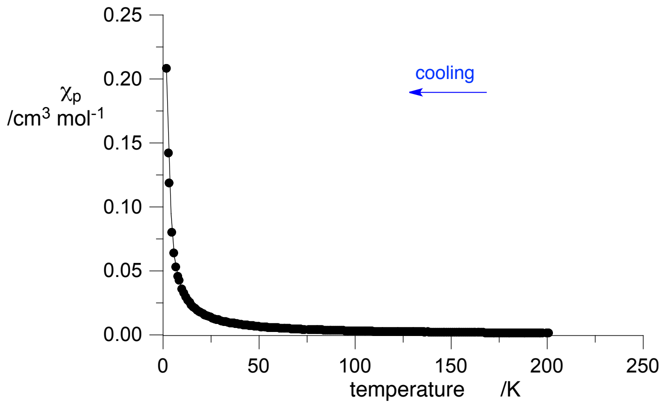

Figure S49. A χ_p *vs* T plot for melted **M[6]** in the cooling mode fitted to Baker's function with C = 0.344 cm^{3}mol^{-1}K. The best-fit functions give J/k_B = 0.422(1) K, r^2 = 0.99997.

Figure S50 shows total molar magnetization in function of applied field B, $M_{tot}(B)$ at selected temperatures.

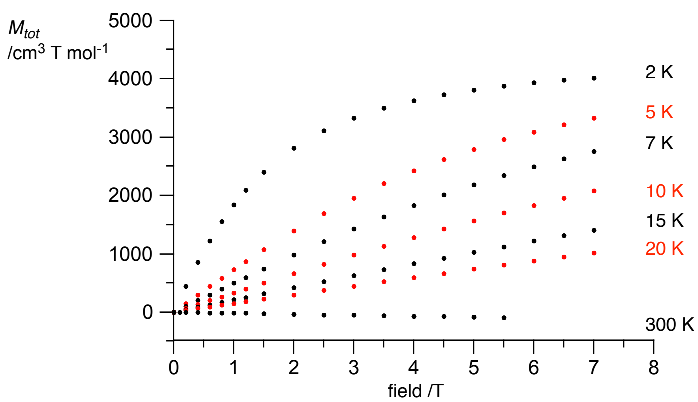

Figure S50. Molar total magnetization M_{mol} *vs* field for solid **M[6]** at selected temperatures.

Monoradical **M[6]**. **melted sample**

m = 16.42 mg, 11.198×10^{-6} mol, M_w= 1466.34 g mol^{-1}

The sample of **M[6]** in a polycarbonate capsule investigated above was briefly heated to 400 K in the magnetometer, cooled to 300 K and analyzed.

Total molar susceptibility, χ, of the sample as a function of temperature in the cooling mode is shown in Figure S51 and a χ•T *vs* T plot in Figure S52.

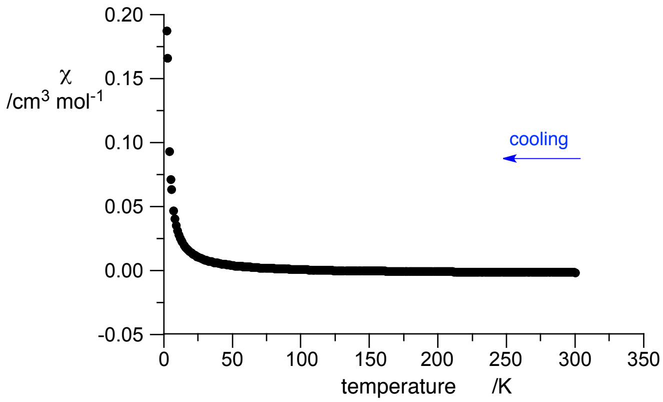

Figure S51. Molar magnetic susceptibility χ *vs* T obtained for melted **M[6]** on cooling 300 K → 2 K at 0.6 T. The heating rate is 1 K/min.

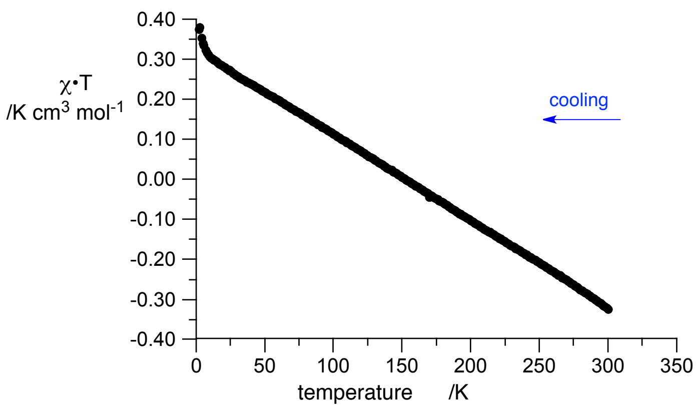

Figure S52. A χ•T *vs* T plot for melted **M[6]** obtained on cooling 300 K → 2 K at 0.6 T. The cooling rate is 1 K/min.

The diamagnetic correction, χ_{dia}, was determined from a linear portion of the χ•T *vs* T plot (Figure S52) in the temperature range 270 K – 200 K (Figure S53).

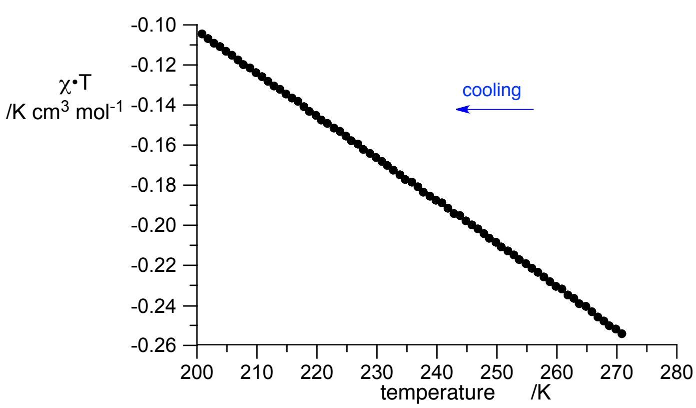

Figure S53. A linear portion of the χ•T *vs* T plot for melted **M[6]** (Figure S52) in a range of 270 K → 200 K. Best fit line: χ•T = -0.002126(2)•T + 0.3223(5), r^2 = 0.9999.

The diamagnetic correction of -0.002126•T cm^{3}mol^{-1}K was applied to the χ•T plot in and the resulting χ_p•T *vs* T plot is shown in Figure S54.

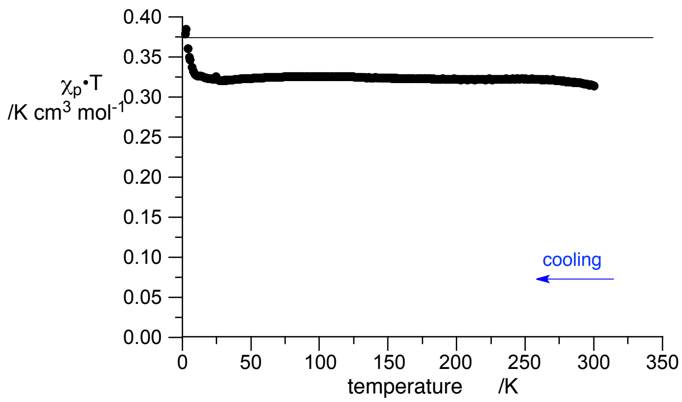

Figure S54. χ_p•T plot *vs* T for melted **M[6]** in the cooling mode after diamagnetic correction χ_{dia} = -0.002126 cm^{3}mol^{-1} determined in Figure S53. The horizontal line marks the value of 0.375 Kcm^{3}mol^{-1} for an ideal paramagnet.

Analysis of the 1/χ_p *vs* T plot in Figure S55 according equation 2 gives the value C = 0.321 cm^{3}mol^{-1}K and the Weiss constant $\theta = +1.1$ K.

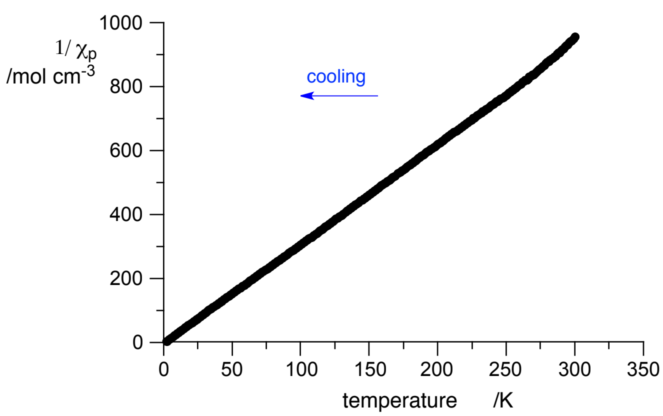

Figure S55. 1/χ_p *vs* T plot for solid **M[6]** in the cooling mode. Best-fit function in the range 50–200 K: 1/χ_p = -3.4(2)+3.113(2)•T, r^2 = 0.9999.

The $\chi_p(T)$ plot (Figure S54) in the temperature range of 2–200 K was fitted to Baker's function (eq. 3b) using Curie constant C established in Figure S55 (C = 0.321 cm^{3}mol^{-1}K) and the result is shown in Figure S56.

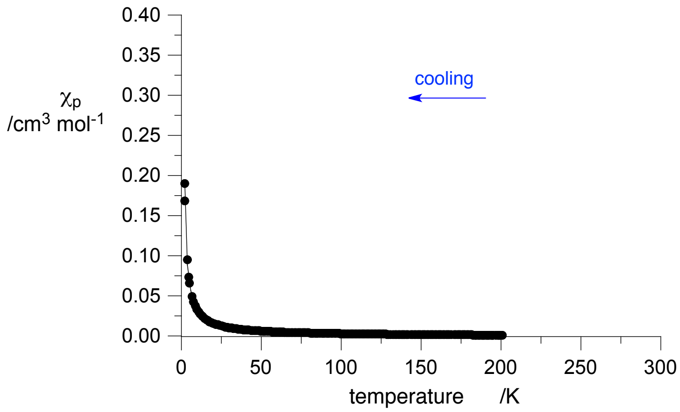

Figure S56. A χ_p *vs* T plot for melted **M[6]** in the cooling mode fitted to Baker's function with C = 0.321 cm^{3}mol^{-1}K. The best-fit functions give J/k_B = 0.403(2) K, r^2 = 0.99997.

Figure S57 shows total molar magnetization in function of applied field B, $M_{tot}(B)$ at selected temperatures.

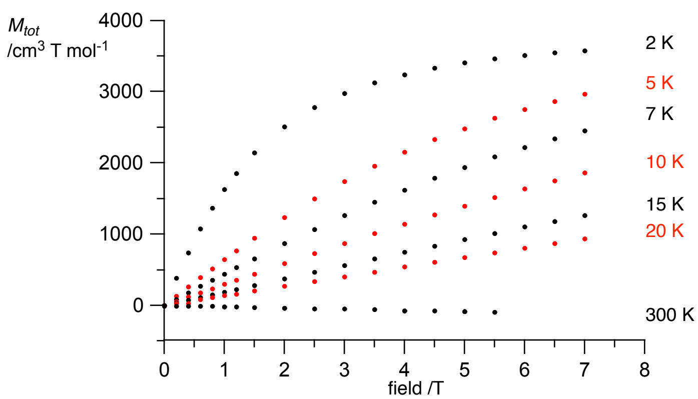

Figure S57. Molar total magnetization M_{mol} *vrs* field for melted **M[6]** at selected temperatures.

Biradicals B[n]

<u>Biradical **B[1]**. **pristine solid sample**</u>

m = 14.56 mg, 9.409×10^{-6} mol/spin, M_w= 1547.39 g mol^{-1} per spin.

Total molar susceptibility, χ, of the sample as a function of temperature in the cooling mode is shown in Figure S58 and a χ•T *vs* T plot in Figure S59.

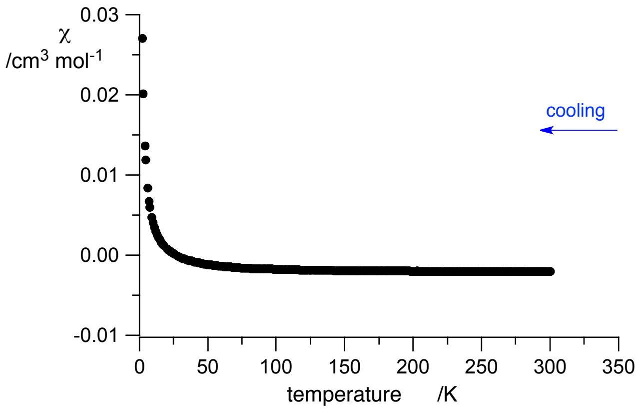

Figure S58. Molar magnetic susceptibility χ *vs* T obtained for pristine sample of **B[1]** on cooling 300 K → 2 K at 0.6 T. The cooling rate is 1 K/min.

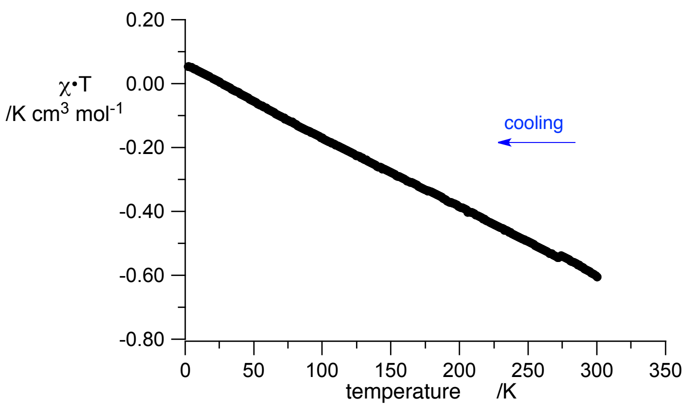

Figure S59. A χ•T *vs* T plot for pristine sample of **B[1]** obtained on cooling 300 K → 2 K at 0.6 T. The cooling rate is 1 K/min.

The diamagnetic correction, χ_{dia}, was determined from a linear portion of the χ•T *vs* T plot (Figure S59) in the temperature range 300 K – 275 K (Figure S60).

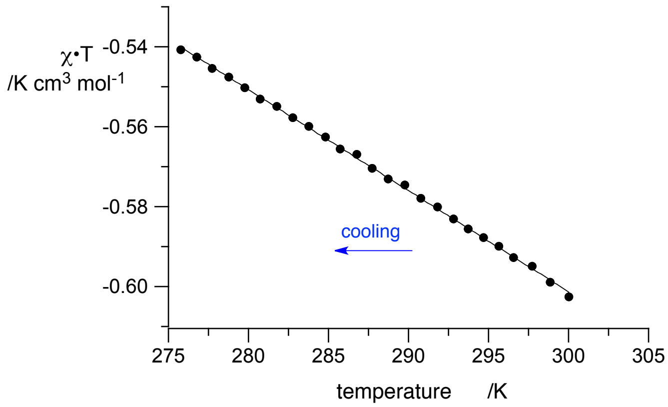

Figure S60. A linear portion of the χ•T *vs* T plot for solid **B[1]** (Figure S59) in the range of 300 K → 275 K. Best fit line: χ•T = -0.002523(14)•T +0.156(4), r^2 = 0.9993.

The diamagnetic correction of -0.002523•T $cm^3mol^{-1}K$ was applied to the χ•T plot and the resulting χ_p•T *vs* T plot is shown in Figure S61.

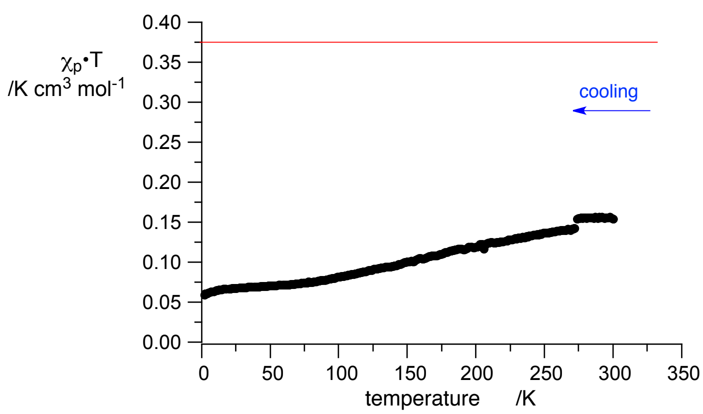

Figure S61. χ_p•T *vs* T plot for solid **B[1]** in the cooling mode after diamagnetic correction of χ_{dia} = -0.002523 cm^3mol^{-1} determined in Figure S60. The horizontal line marks the value of 0.375 Kcm^3mol^{-1} for an ideal paramagnet.

The 1/χ_p *vs* T plot for solid **B[1]** has two distinct linear regions shown in Figure S62. It was analyzed according to equation 2.

The upper temperature region (140-260 K): C = 0.294 Kcm^3mol^{-1} and θ = -289 K.

The lower temperature region (20-70 K): C = 0.076 Kcm^3mol^{-1} and θ = -3.5 K.

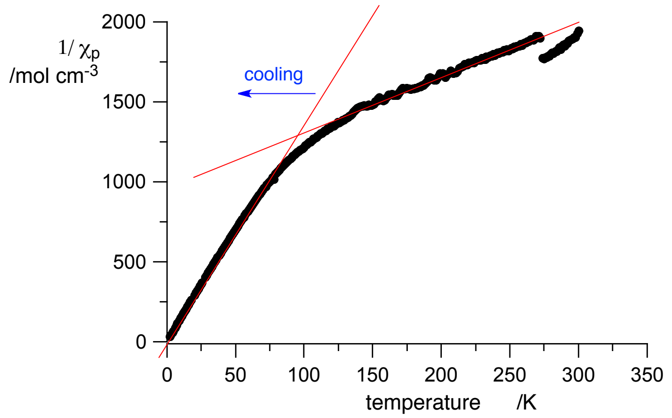

Figure S62. 1/χ_p *vs* T plot for solid **B[1]** in the cooling mode.

Figure S63 shows total molar magnetization in function of applied field B, $M_{tot}(B)$, in selected temperatures.

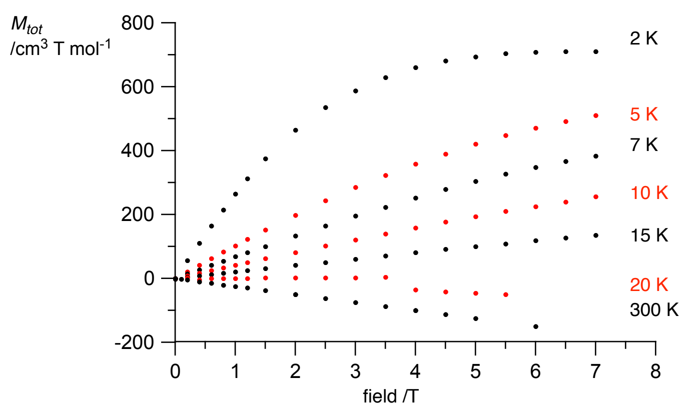

Figure S63. Molar total magnetization M_{mol} *vs* field for solid **B[1]** at selected temperatures.

Biradical **B[1]**. **melted sample**

A fresh sample of **B[1]** was briefly heated on a glass substrate to *ca* 150 ºC, quickly cooled (quenched) and transferred to a polycarbonate capsule.

m = 6.095 mg, 3.939×10^{-6} mol/spin, M_w= 1547.39 g mol^{-1} per spin.

Total molar susceptibility, χ, of the sample as a function of temperature in the cooling mode is shown in Figure S64 and a χ•T *vs* T plot in Figure S65.

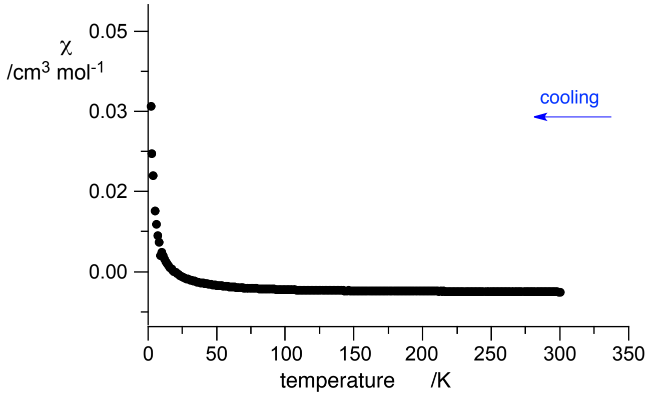

Figure S64. Molar magnetic susceptibility χ *vs* T obtained for melted sample of **B[1]** on cooling 300 K → 2 K at 0.6 T. The cooling rate is 1 K/min.

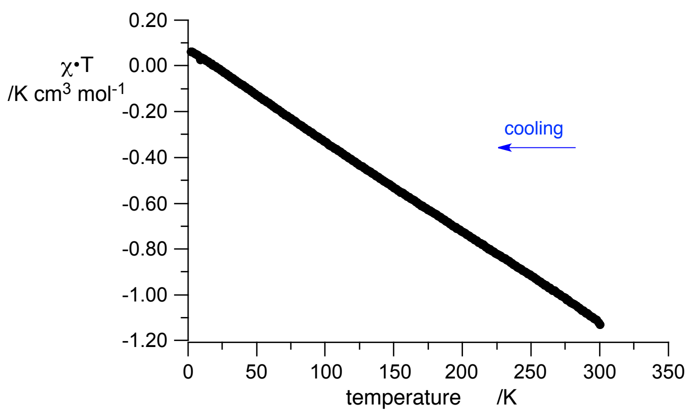

Figure S65. A χ•T *vs* T plot for melted **B[1]** obtained on cooling 300 K → 2 K at 0.6 T. The cooling rate is 1 K/min.

The diamagnetic correction, χ_{dia}, was determined from a linear portion of the χ•T *vs* T plot (Figure S65) in the temperature range 300 K – 200 K (Figure S66).

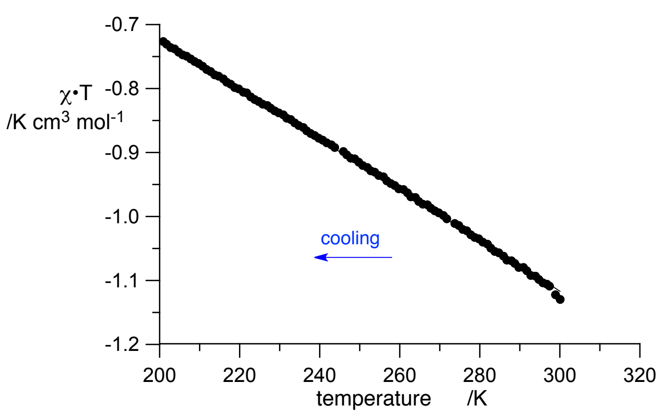

Figure S66. A linear portion of the χ•T *vs* T plot for melted **B[1]** in the range of 300 K → 200 K. Best fit line: χ•T = -0.003947(9)•T +0.068(2), r^2 = 0.9995.

The diamagnetic correction of -0.003947•T cm^{3}mol^{-1}K was applied to the χ•T plot and the resulting χ_p•T *vs* T plot is shown in Figure S67.

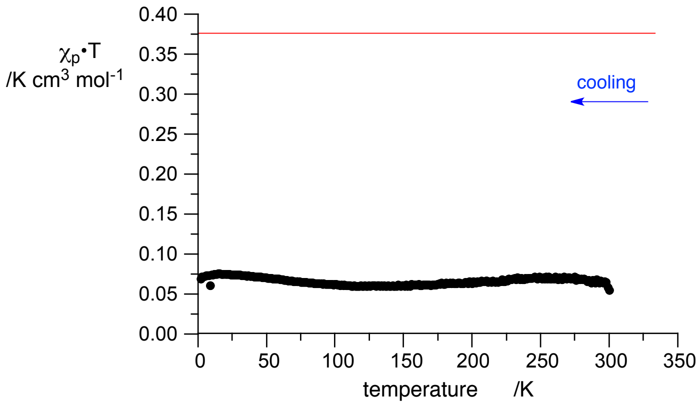

Figure S67. χ_p•T *vs* T plot in the cooling mode for melted **B[1]** after diamagnetic correction χ_{dia} = -0.003947 cm^{3}mol^{-1}) determined in Figure S66. The horizontal line marks the value of 0.375 Kcm^{3}mol^{-1} for an ideal paramagnet.

The 1/χ_p *vs* T plot for melted **B[1]** shown in Figure S68 does not allow for Curie-Weiss analysis.

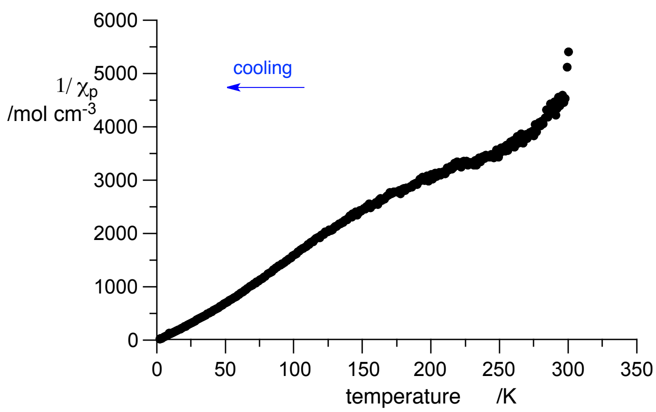

Figure S68. 1/χ_p *vs* T plot for melted **B[1]** in the cooling mode.

Figure S69 shows the total molar magnetization in function of applied field B, $M_{tot}(B)$, in selected temperatures. A comparison of χ_p•T (T) plots for pristine and melted samples of **B[1]** is shown in Figure S70.

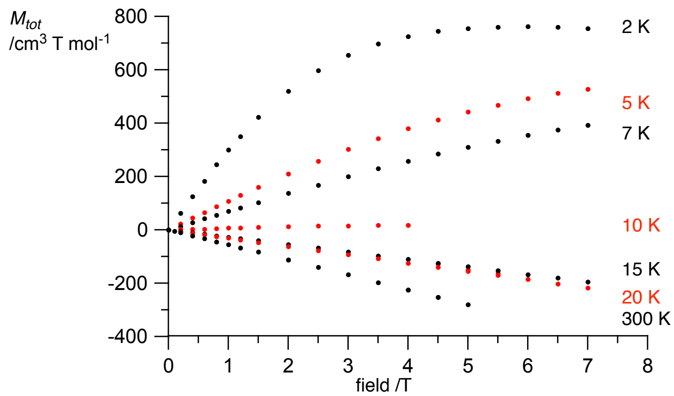

Figure S69. Molar total magnetization M_{mol} *vs* field for solid **B[1]** at selected temperatures.

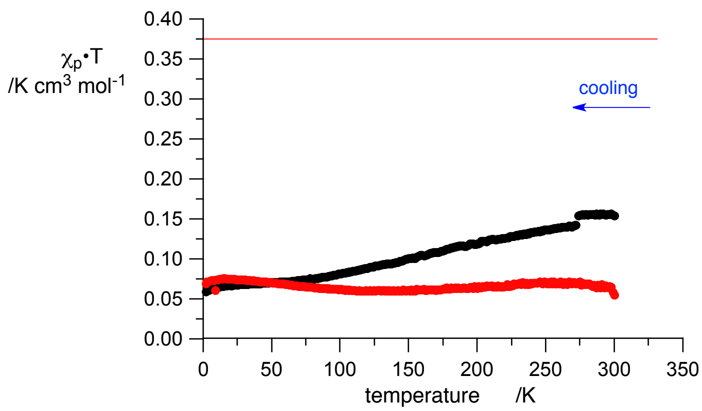

Figure S70. χ_p•T *vs* T plots for solid (black) and melted (red) sample of **B[1]** in the cooling mode. The horizontal line marks the value of 0.375 Kcm^3mol^{-1} for an ideal paramagnet.

Biradical **B[3]**. **pristine solid sample**

m = 13.63 mg, $8.808{\times}10^{-6}$ mol/spin, M_w= 1547.39 g mol^{-1} per spin.

Total molar susceptibility, χ, of the sample as a function of temperature in the cooling mode is shown in Figure S71 and a χ•T *vs* T plot in Figure S72.

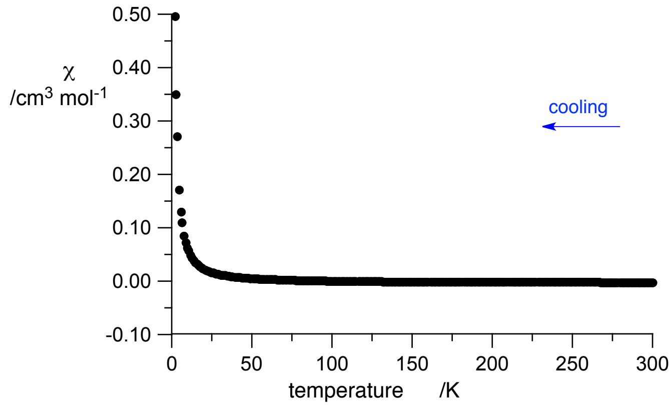

Figure S71. Molar magnetic susceptibility χ *vs* T obtained for solid **B[3]** on cooling 300 K → 2 K at 0.6 T. The cooling rate is 1 K/min.

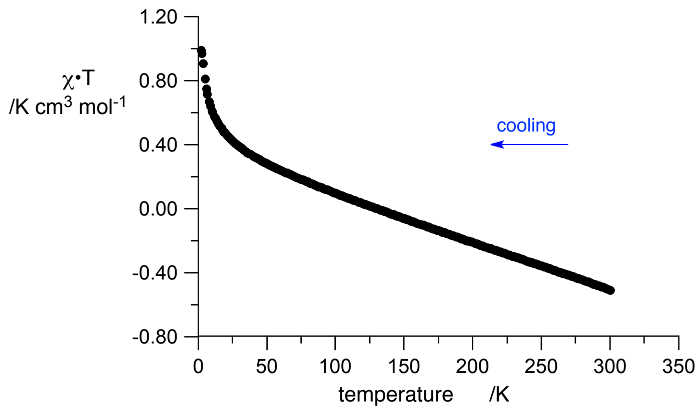

Figure S72. A χ•T *vs* T plot for solid **B[3]** obtained on cooling 300 K → 2 K at 0.6 T. The cooling rate is 1 K/min.

The diamagnetic correction, χ_{dia}, was determined from a linear portion of the χ•T *vs* T plot (Figure S72) in the temperature range 300 K – 200 K (Figure S73).

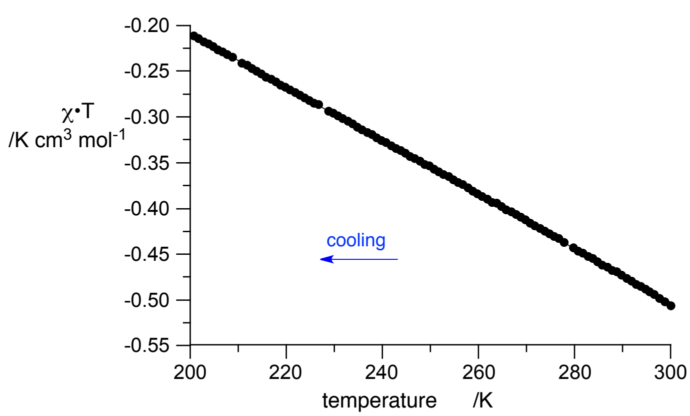

Figure S73. A linear portion of the χ•T *vs* T plot for solid **B[3]** (Figure S72) in the range of 200 K → 300 K. Best fit line: χ•T = -0.002938(3)•T + 0.3790(9), r^2 = 0.9999.

The diamagnetic correction of -0.002938•T cm^{3}mol^{-1}K was applied to the χ•T plot and the resulting χ_p•T *vs* T plot is shown in Figure S74, while the 1/χ_p *vs* T plot in Figure S75.

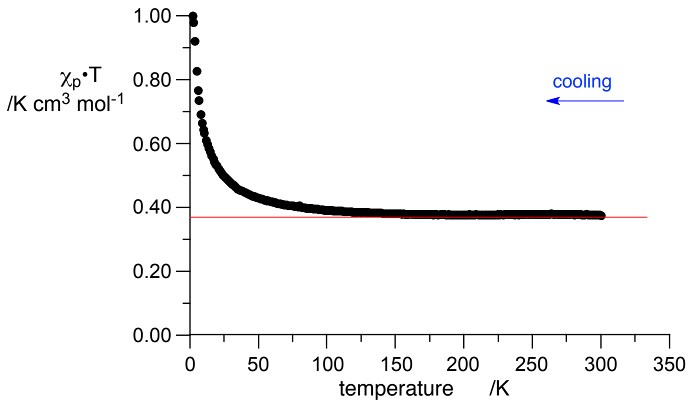

Figure S74. χ_p•T *vs* T plot for solid **B[3]** in the cooling mode after diamagnetic correction χ_{dia} = -0.002938 cm^{3}mol^{-1} determined in Figure S73.

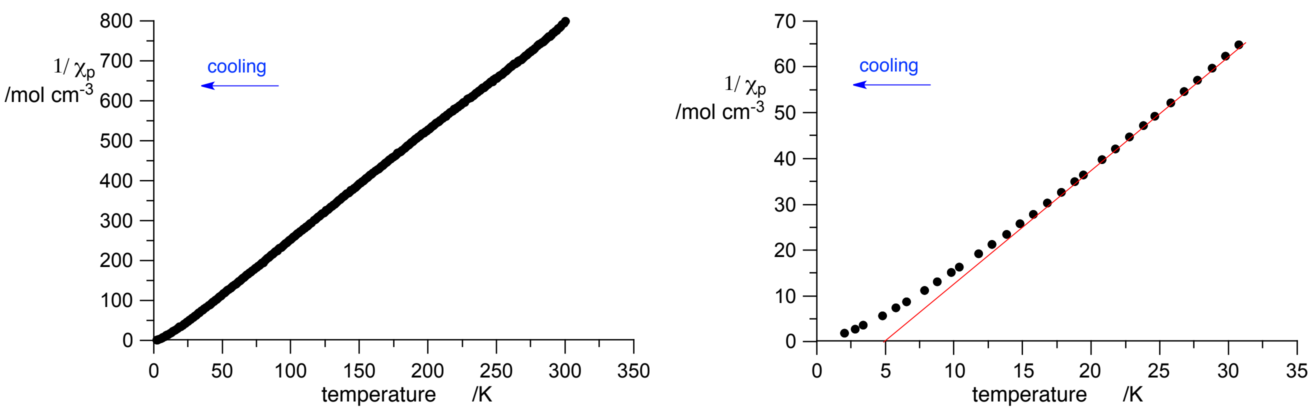

Figure S75. 1/χ_p *vs* T plot for solid **B[3]** in the cooling mode. Best fit function in the range 50–200 K: 1/χ_p = -21.4(2)+2.759(1)•T, r^2 = 0.9999.

Analysis of the 1/χ_p *vs* T plot in the range of 50–200 K for solid **B[3]** according to equation 2 gives the value C = 0.362 cm^{3}mol^{-1}K and the Weiss constant θ = +7.76 K.

The $\chi_p(T)$ plot (Figure S74) in the temperature range of 2–200 K was fitted to Baker's function (eq. 3b) using Curie constant C established in Figure S75 (C = 0.362 cm^{3}mol^{-1}K) and the result is shown in Figure S76.

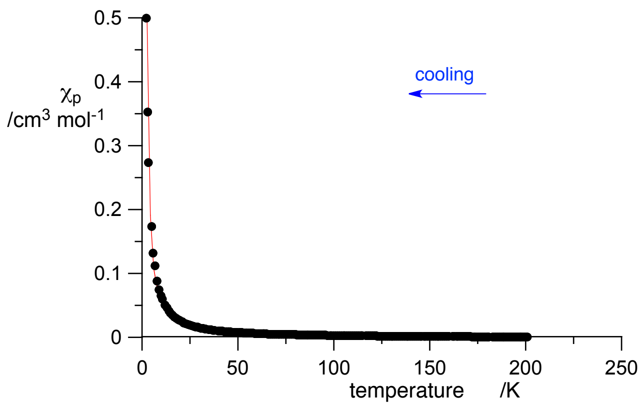

Figure S76. A χ_p *vs* T plot for **B[3]** in the cooling mode fitted to Baker's function with $C = 0.362$. The best-fit function give $J/k_B = 5.48(8)$ K, $r^2 = 0.991$

Figure S77 shows total molar magnetization in function of applied field B, $M_{tot}(B)$ at selected temperatures.

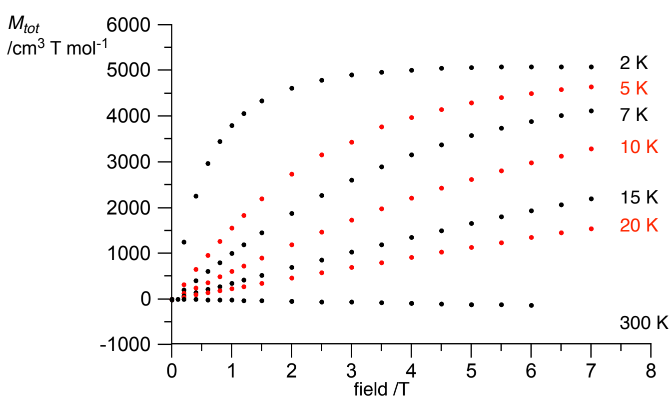

Figure S77. Molar total magnetization M_{mol} *vrs* field for solid **B[3]** at selected temperatures.

<u>Biradical **B[3]**. **melted sample**</u>

A fresh sample of **B[3]** was briefly heated on a glass plate to *ca* 150 °C, quickly cooled (quenched) and transferred to a polycarbonate capsule.

m = 7.96 mg, 5.144×10^{-6} mol/spin, M_w= 1547.39 g mol^{-1} per spin.

Total molar susceptibility, χ, of the sample as a function of temperature in the cooling mode is shown in Figure S78 and a χ•T *vs* T plot in Figure S79.

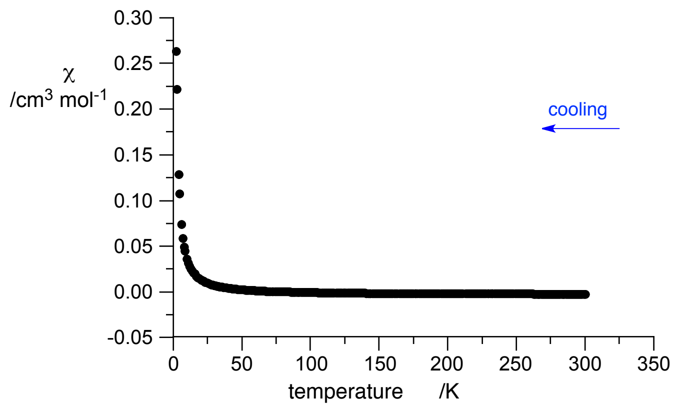

Figure S78. Molar magnetic susceptibility χ *vs* T obtained for melted sample of **B[3]** on cooling 300 K → 2 K at 0.6 T. The cooling rate is 1 K/min.

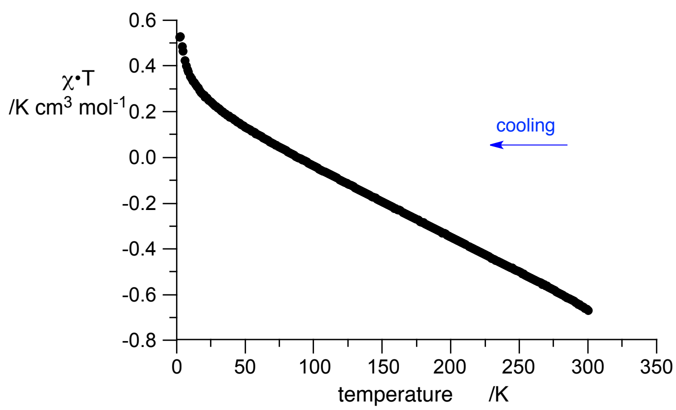

Figure S79. A χ•T *vs* T plot for melted sample of **B[3]** obtained on cooling 300 K → 2 K at 0.6 T. The cooling rate is 1 K/min.

The diamagnetic correction, χ_{dia}, was determined from a linear portion of the χ•T *vs* T plot (Figure S79) in the temperature range 300 K – 200 K (Figure S80).

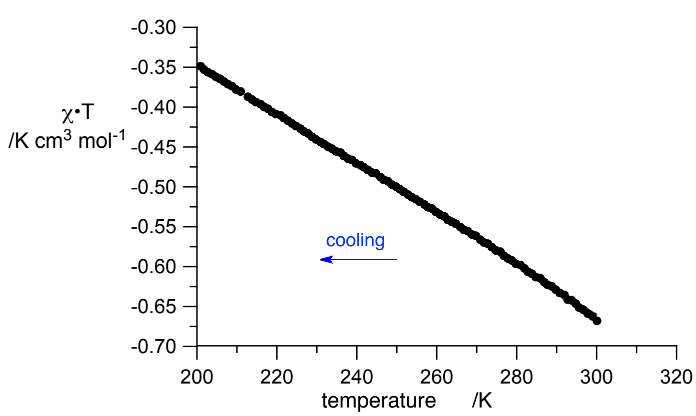

Figure S80. A linear portion of the χ•T *vs* T plot for melted **B[3]** (Figure S79) in the range of 300 K → 200 K. Best fit line: χ•T = -0.003140(7)•T +0.283(2), r^2 = 0.9995.

The diamagnetic correction of -0.003140•T $cm^3mol^{-1}K$ was applied to the χ•T plot and the resulting χ_p•T *vs* T plot is shown in Figure S81, while the $1/\chi_p$ *vs* T plot in Figure S82.

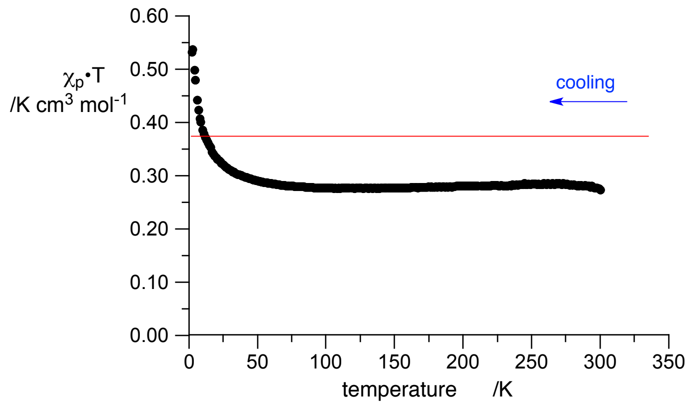

Figure S81. χ_p•T *vs* T plot for melted **B[3]** in the cooling mode after diamagnetic correction χ_{dia} = -0.003140 cm^3mol^{-1} determined in Figure S80. The horizontal line marks the value of 0.375 Kcm^3mol^{-1} for an ideal paramagnet.

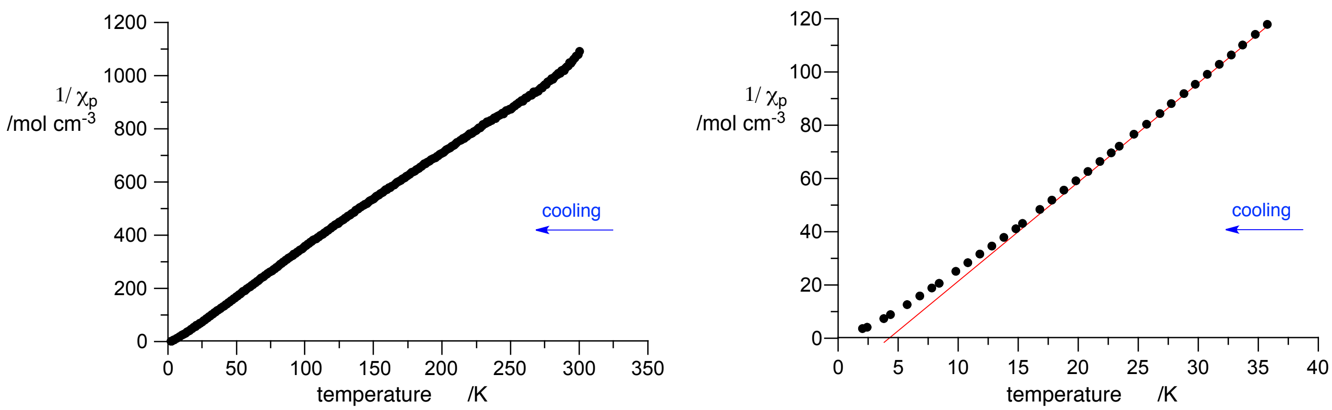

Figure S82. $1/\chi_p$ *vs* T plot for melted **B[3]**. Best fit function in the range 50–200 K:
$1/\chi_p$ = -1.89(2)+3.600(6)•T, r^2 = 0.9996.

Analysis of the $1/\chi_p$ *vs* T plot according to equation 2 gives the value C = 0.278 $cm^3mol^{-1}K$ and the Weiss constant θ = +0.53 K.

The $\chi_p(T)$ plot (Figure S81) in the temperature range of 2–200 K was fitted to Baker's function (eq. 3b) using Curie constant C established in Figure S82 (C = 0.278 $cm^3mol^{-1}K$) and the result is shown in Figure S83.

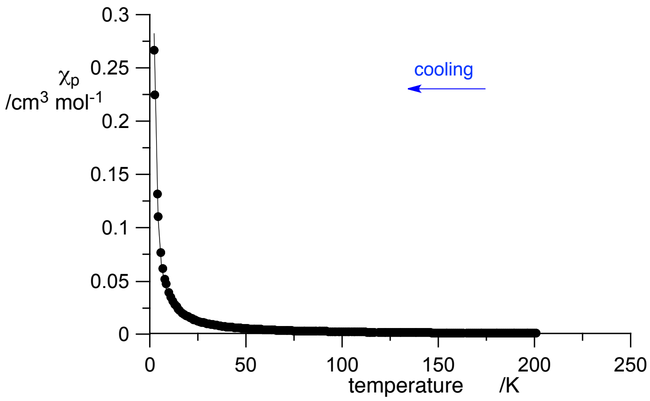

Figure S83. A χ_p *vs* T plot for melted **B[3]** in the cooling mode fitted to Baker's function with C = 0.278 (Figure S81). The best-fit functions give J/k_B = 2.46(4) K, r^2 = 0.994.

A comparison of χ_p•T (T) plots for pristine and melted samples of **B[3]** are shown in Figure S84.

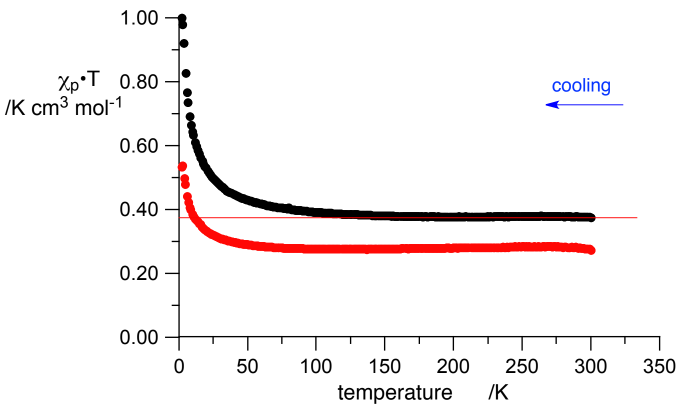

Figure S84. χ_p•T *vs* T plots for solid (black) and melted (red) sample of **B[3]** in the cooling mode. The horizontal line marks the value of 0.375 Kcm^{3}mol^{-1} for an ideal paramagnet.

Figure S85 shows total molar magnetization in function of applied field B, $M_{tot}(B)$ at selected temperatures.

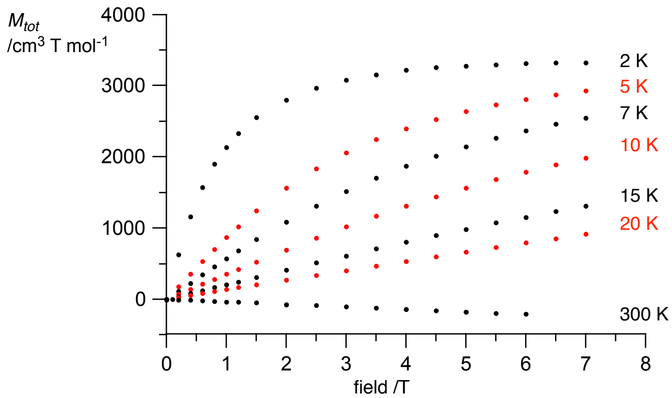

Figure S85. Molar total magnetization M_{mol} *vrs* field for melted **B[3]** at selected temperatures.

Biradical **B[6]**. **pristine solid sample**

m = 18.81 mg, 12.156×10^{-6} mol/spin, M_w= 1547.39 g mol^{-1} per spin.

Total molar susceptibility, χ, of the sample as a function of temperature in the cooling mode is shown in Figure S86 and a χ•T *vs* T plot in Figure S87.

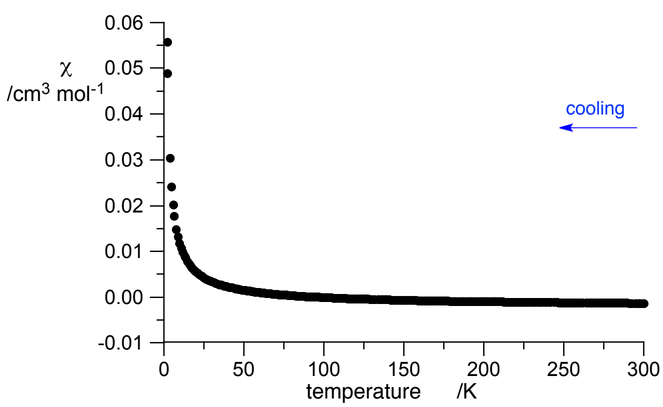

Figure S86. Molar magnetic susceptibility χ *vs* T obtained for solid **B[6]** on cooling 300 K → 2 K at 0.6 T. The cooling rate is 1 K/min.

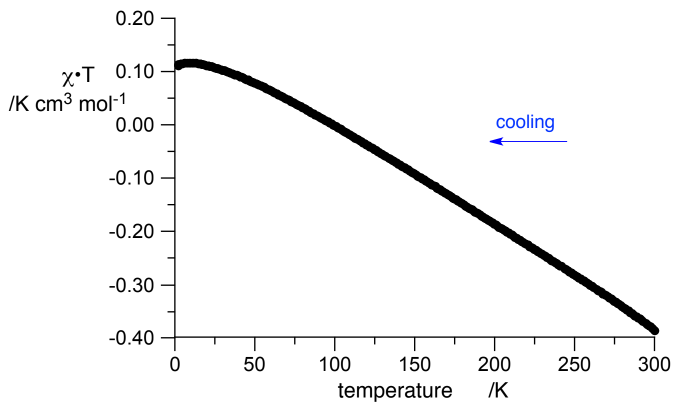

Figure S87. A χ•T *vs* T plot for solid **B[6]** obtained on cooling 300 K → 2 K at 0.6 T. The cooling rate is 1 K/min.

The diamagnetic correction, χ_{dia}, was determined from a linear portion of the χ•T *vs* T plot (Figure S87) in the temperature range 297 K – 272 K (Figure S88).

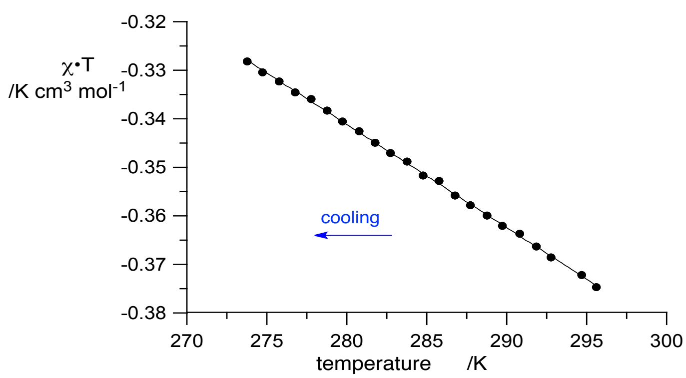

Figure S88. A linear portion of the χ•T *vs* T plot for **B[6]** (Figure S87) in the range of 297 K → 272 K. Best fit line: χ•T = -0.002121(10)•T + 0.253(3), r^2 = 0.9996.

The diamagnetic correction of -0.002121•T $cm^3mol^{-1}K$ was applied to the χ•T plot in and the resulting χ_p•T *vs* T plot is shown in Figure S89, while the $1/\chi_p$ *vs* T plot is shown in Figure S90.

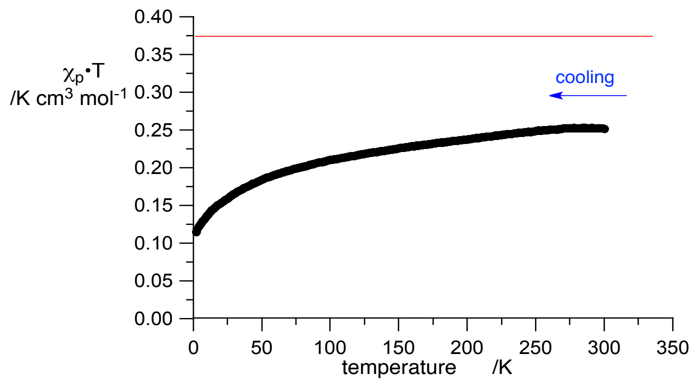

Figure S89. χ_p•T plot *vs* T for solid **B[6]** in the cooling mode after diamagnetic correction of χ_{dia} = -0.002121 cm^{3}mol^{-1}, determined in Figure S88. The horizontal line marks the value of 0.375 Kcm^{3}mol^{-1} for an ideal paramagnet.

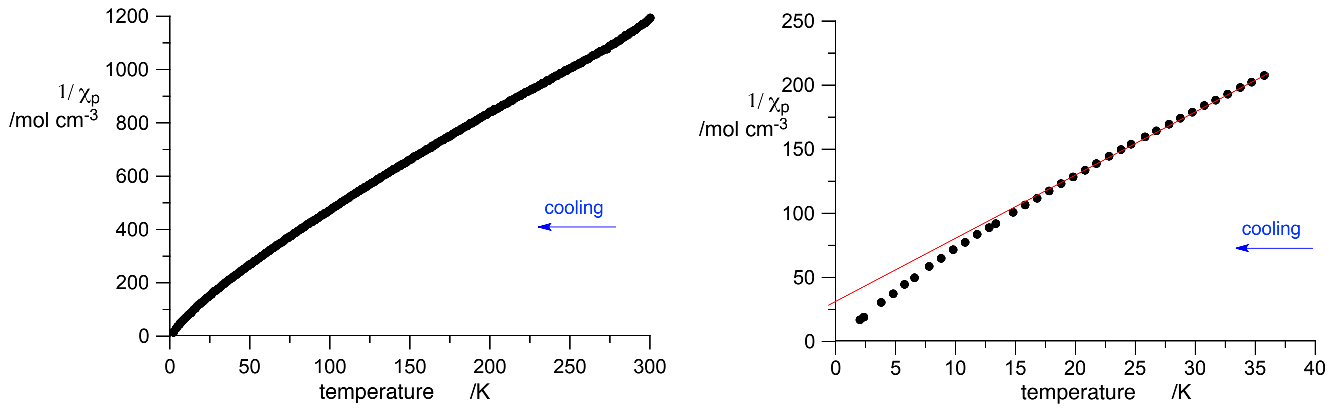

Figure S90. 1/χ_p plot *vs* T for **B[6]** in the cooling mode. Best fit functions in the range 100–250 K: 1/χ_p = 133(1)+3.521(7)•T, r^2 = 0.9993 for cooling.

Analysis of the 1/χ_p *vs* T plot for solid **B[6]** in Figure S90 according to equation 2 gives the value C = 0.284 cm^{3}mol^{-1}K and the Weiss constant θ = -37.8 K.

Figure S91 shows total molar magnetization in function of applied field B, $M_{tot}(B)$ at selected temperatures.

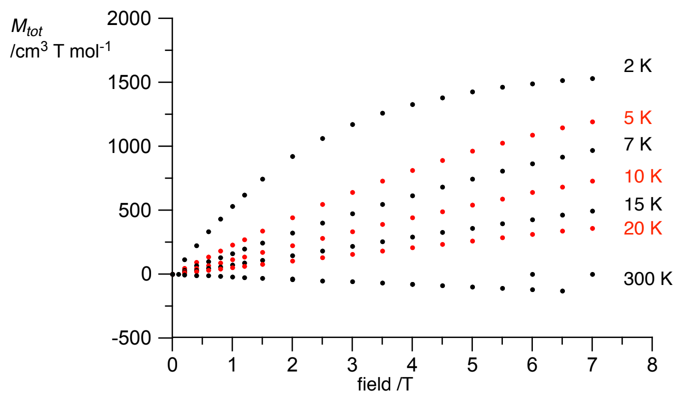

Figure S91. Molar total magnetization M_{mol} *vrs* field for solid **B[6]** at selected temperatures.

Biradical **B[6]**. **melted sample**

A sample of **B[6]** was briefly heated on a glass plate to *ca* 150 ºC, quickly cooled (quenched) and transferred to a polycarbonate capsule.

m = 7.99 mg, 5.1635×10^{-6} mol/spin, M_w= 1547.39 g mol^{-1} per spin.

Total molar susceptibility, χ, of the sample as a function of temperature in the cooling mode is shown in Figure S92 and a χ•T *vs* T plot in Figure S93.

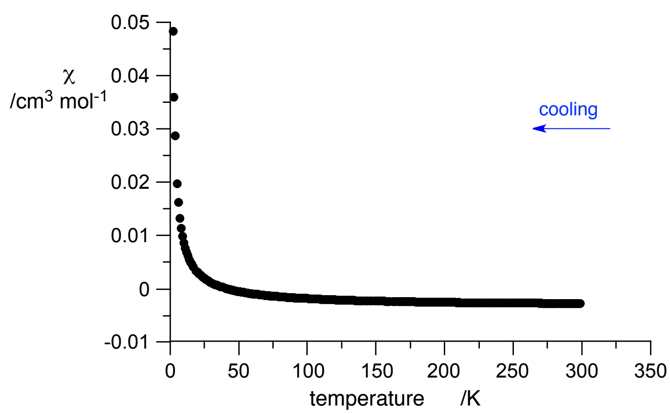

Figure S92. Molar magnetic susceptibility χ *vs* T obtained for melted sample of **B[6]** on cooling 300 K → 2 K at 0.6 T. The cooling rate is 1 K/min.

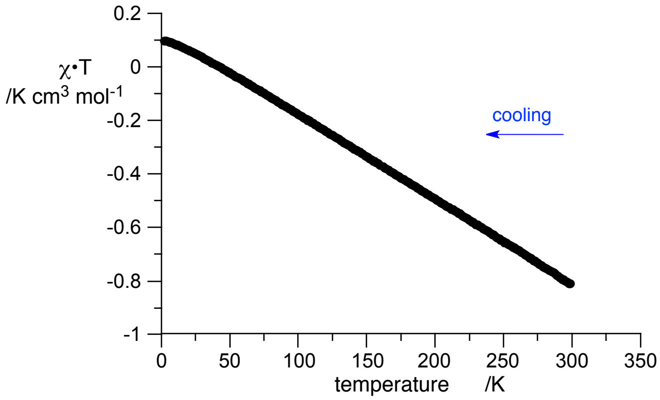

Figure S93. A χ•T *vs* T plot for melted sample of **B[6]** obtained on cooling 300 K → 2 K at 0.6 T. The cooling rate is 1 K/min.

The diamagnetic correction, χ_{dia}, was determined from a linear portion of the χ•T *vs* T plot (Figure S93) in the temperature range 300 K – 200 K (Figure S94).

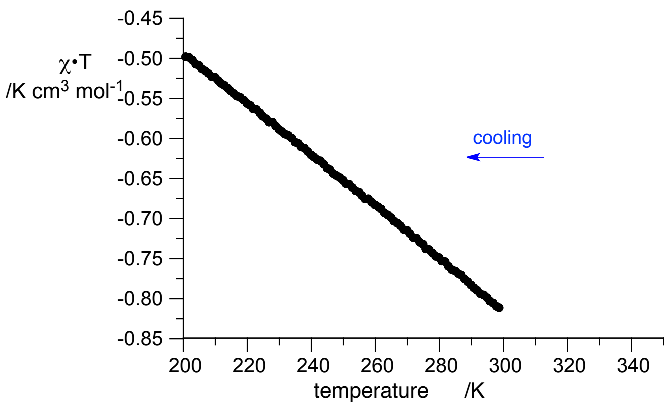

Figure S94. A linear portion of the χ•T *vs* T plot for melted **B[6]** (Figure S93) in the range of 300 K → 200 K. Best fit line: χ•T = -0.003214(5)•T +0.1507(12), r^2 = 0.9998.

The diamagnetic correction of -0.003214•T $cm^3mol^{-1}K$ was applied to the χ•T and the resulting χ_p•T *vs* T plot is shown in Figure S95, while the 1/χ_p *vs* T plot in Figure S96.

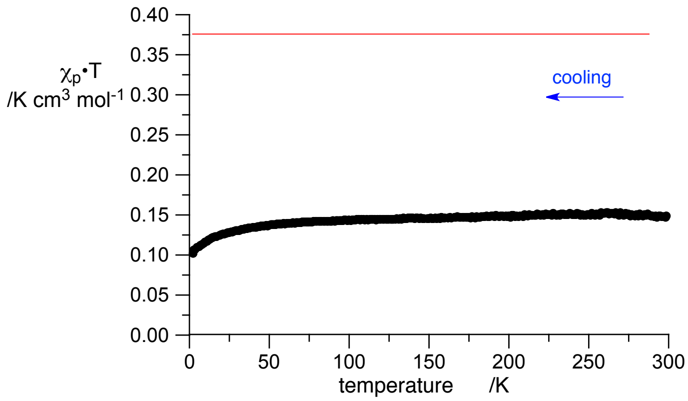

Figure S95. χ_p•T *vs* T plot for melted **B[6]** after diamagnetic correction χ_{dia} = -0.003214 cm^{3}mol^{-1} determined in Figure S94. The horizontal line marks the value of 0.375 Kcm^{3}mol^{-1} for an ideal paramagnet.

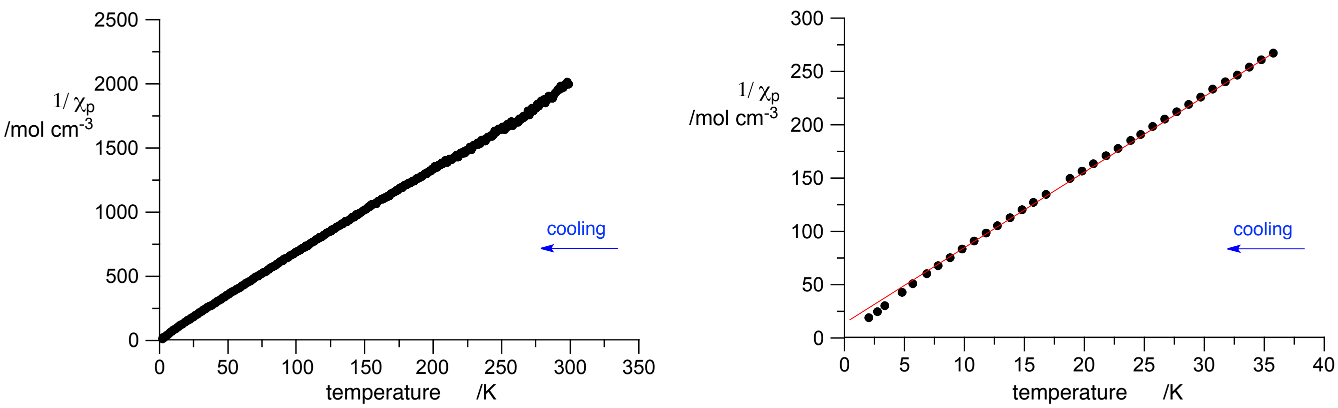

Figure S96. 1/χ_p plot *vs* T for melted **B[6]**. Best fit function in the range 100–250 K:

$1/\chi_p$ = 67(2)+6.35(1)•T, r^2 = 0.9994.

Analysis of the 1/χ_p *vs* T plot in Figure S96 according equation 2 gives the value C = 0.157 cm^{3}mol^{-1}K and the Weiss constant $\theta = -10.5$ K.

Figure S97 shows total molar magnetization in function of applied field B, $M_{tot}(B)$ at selected temperatures.

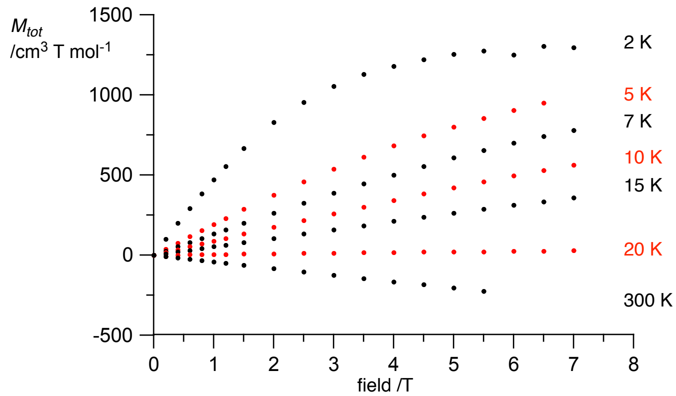

Figure S97. Molar total magnetization M_{mol} *vrs* field for melted **B[6]** at selected temperatures.

A comparison of χ_p•T (T) plots for pristine and melted samples of **B[6]** is shown in Figure S98.

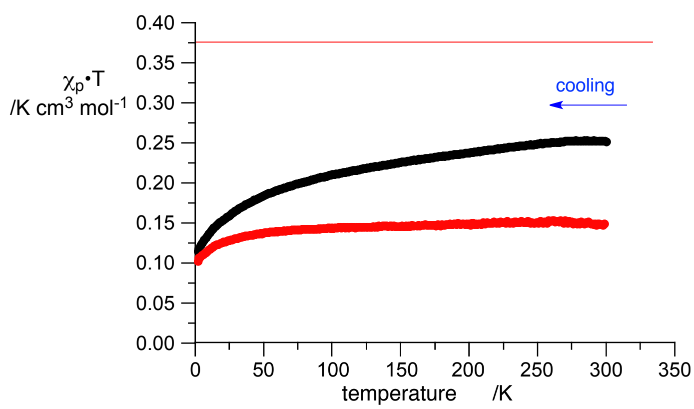

Figure S98. χ_p•T *vs* T plots for solid (black) and melted (red) sample of **B[6]**. The horizontal line marks the value of 0.375 Kcm^{3}mol^{-1} for an ideal paramagnet.

Triradicals T[n]

Triradical **T[1]**. **pristine solid sample**

m = 23.97 mg, 15.622×10^{-6} mol/spin, M_w= 1534.37 g mol^{-1} per spin.

Total molar susceptibility, χ, of the sample as a function of temperature in the cooling mode is shown in Figure S99 and a χ•T *vs* T plot in Figure S100.

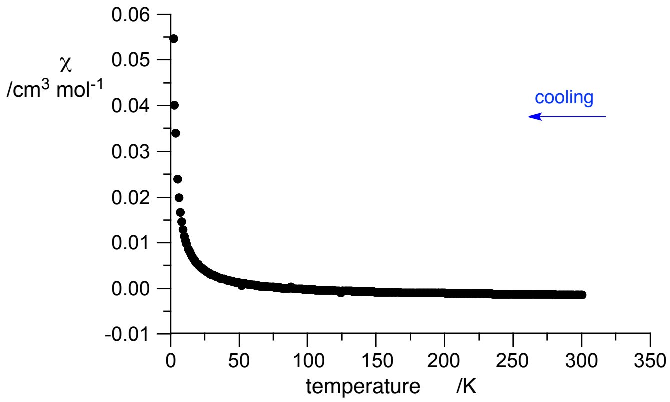

Figure S99. Molar magnetic susceptibility χ *vs* T obtained for solid **T[1]** on cooling 300 K → 2 K at 0.6 T. The cooling rate is 1 K/min.

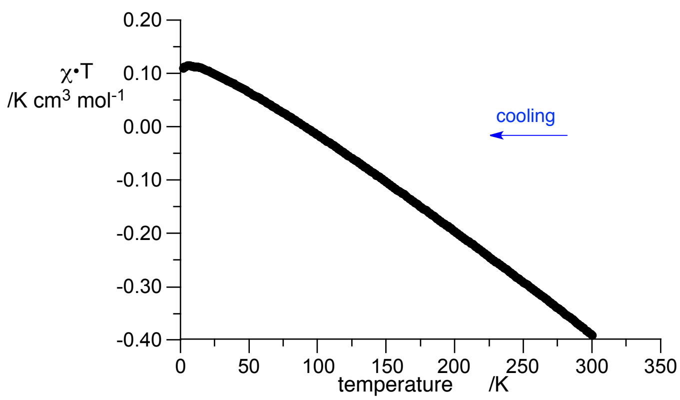

Figure S100. A χ•T *vs* T plot for solid **T[1]** obtained on cooling 300 K → 2 K at 0.6 T. The cooling rate is 1 K/min.

The diamagnetic correction, χ_{dia}, was determined from a linear portion of the χ•T *vs* T plot (Figure S100) in the temperature range 300 K – 200 K (Figure S101).

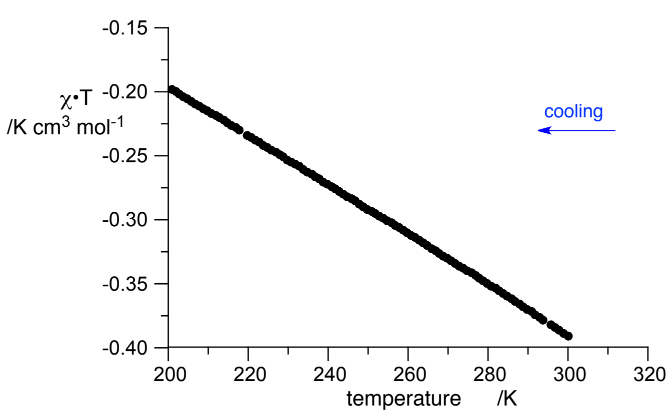

Figure S101. A linear portion of the χ•T *vs* T plot for solid **T[1]** (Figure S100) in the range of 200 K → 300 K. Best fit line: χ•T = -0.001932(2)•T + 0.1910(6), r^2 = 0.9999.

The diamagnetic correction of -0.001932•T cm^{3}mol^{-1}K was applied to the χ•T plot in and the resulting χ_p•T *vs* T plot is shown in Figure S102.

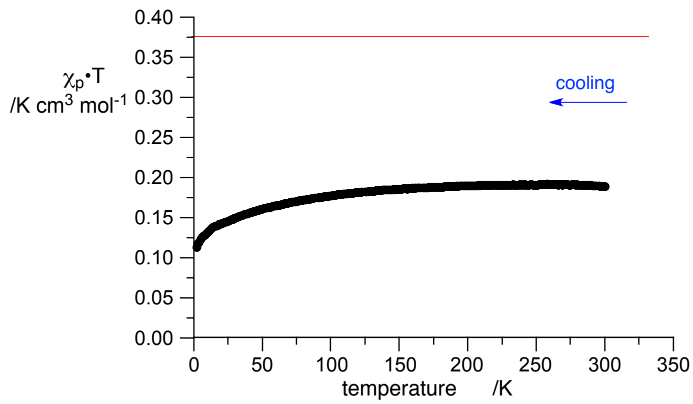

Figure S102. χ_p•T plot *vs* T for solid **T[1]** in the cooling mode after diamagnetic correction χ_{dia} = -0.001932 cm^{3}mol^{-1}, determined in Figure S101. The horizontal line marks the value of 0.375 Kcm^{3}mol^{-1} for an ideal paramagnet.

The 1/χ_p *vs* T plot for solid **T[1]** is shown in Figure S103.

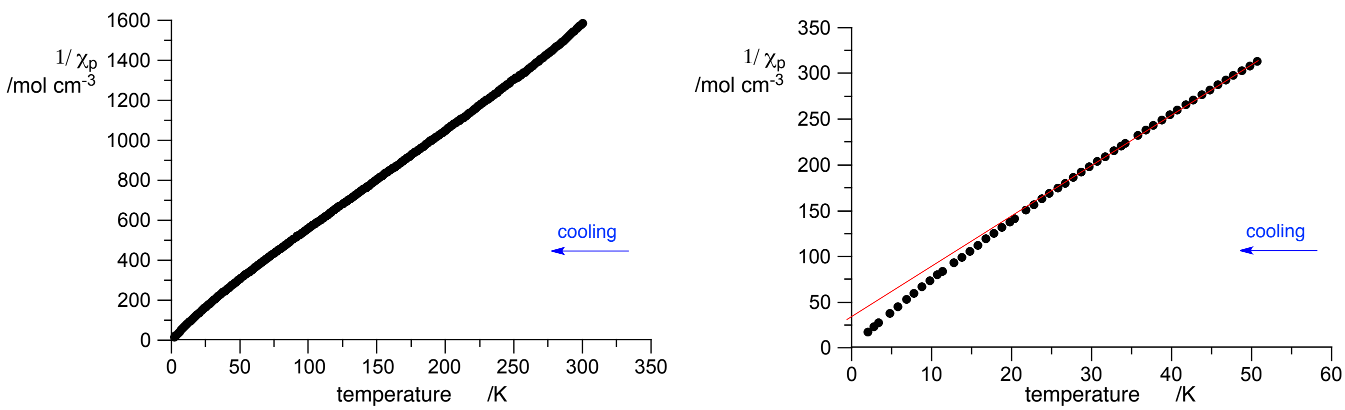

Figure S103. 1/χ_p plot *vs* T for solid **T[1]** in the cooling mode. Best fit functions in the range 100–250 K: 1/χ_p = 65.3(6)+4.944(4)•T, r^2 = 0.9999 for cooling.

Analysis of the 1/χ_p *vs* T plot for solid **T[1]** in Figure S103 according to equation 2 gives the value C = 0.202 cm^{3}mol^{-1}K and the Weiss constant $\theta = -13.2$ K.

Figure S104 shows total molar magnetization in function of applied field B, $M_{tot}(B)$, in selected temperatures.

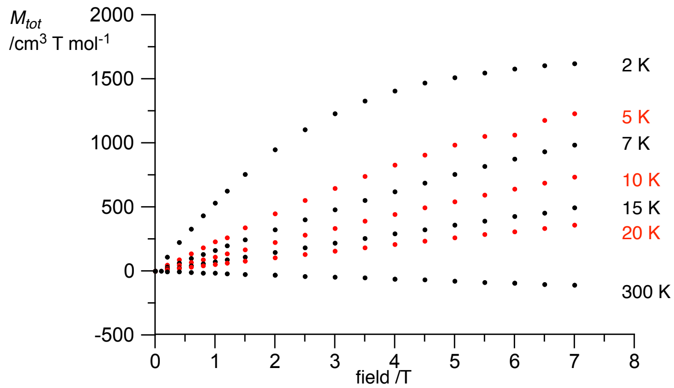

Figure S104. Molar total magnetization M_{mol} *vs* field for solid **T[1]** at selected temperatures.

Triradical **T[1]**. **melted sample**

A fresh sample of **T[1]** was briefly heated on a glass plate to *ca* 150 °C quickly cooled (quenched) and transferred to a polycarbonate capsule.

m = 15.00 mg, 9.776×10^{-6} mol/spin, M_w= 1534.37 g mol^{-1} per spin.

Total molar susceptibility, χ, of the melted sample as a function of temperature in the cooling cycle is shown in Figure S105 and a χ•T *vs* T plot in Figure S106.

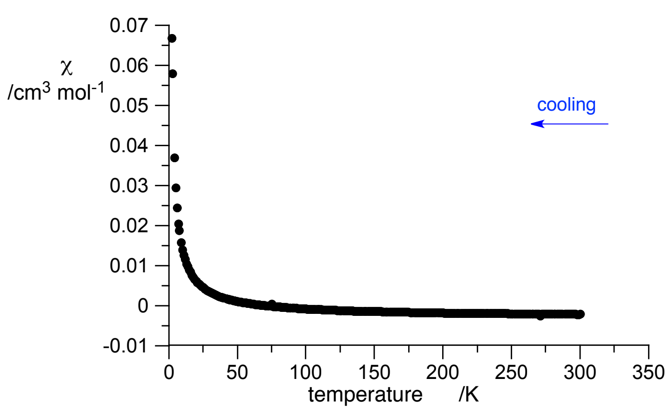

Figure S105. Molar magnetic susceptibility χ *vs* T obtained for melted **T[1]** in the cooling cycle 300 K → 2 K at 0.6 T. The cooling rate is 1 K/min.

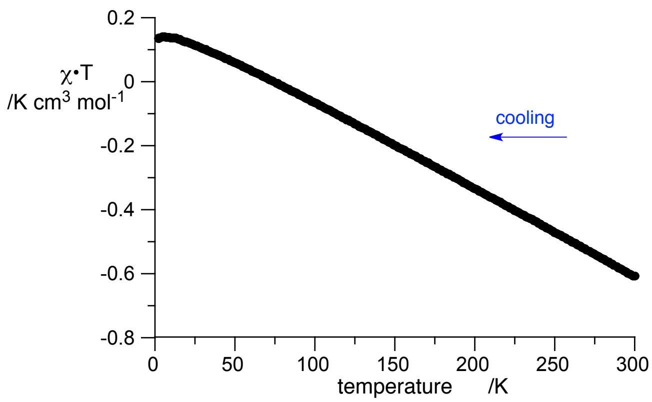

Figure S106. A χ•T *vs* T plot for melted **T[1]** obtained in the cooling cycle 300 K → 2 K at 0.6 T. The cooling rate is 1 K/min.

The diamagnetic correction, χ_{dia}, was determined from a linear portion of the χ•T *vs* T plot (Figure S106) in the temperature range 300 K – 200 K (Figure S107).

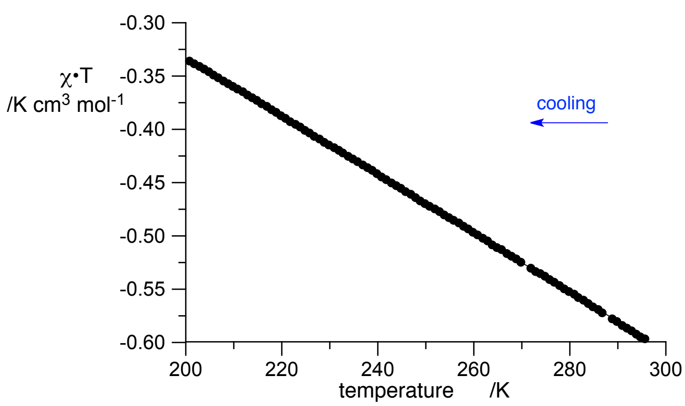

Figure S107. A linear portion of the χ•T *vs* T plot for melted **T[1]** (Figure S106) in the range of 200 K → 295 K. Best fit line: χ•T = –0.002750(2)•T + 0.2177(5), r^2 = 0.99995.

The diamagnetic correction of -0.002750•T $cm^3 mol^{-1}K$ was applied to the χ•T plot and the resulting χ_p•T *vs* T plot is shown in Figure S108, while the 1/χ_p *vs* T plot in Figure S109.

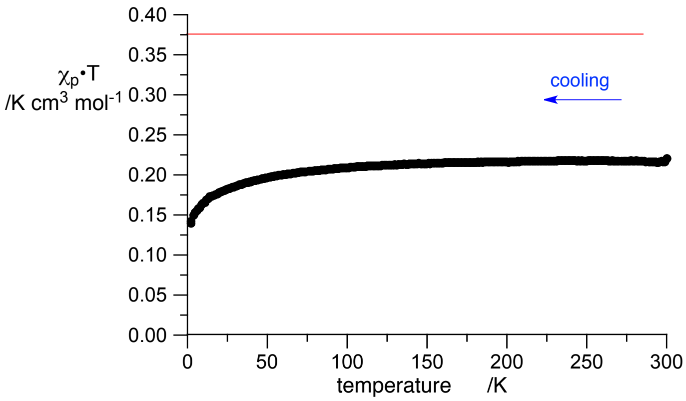

Figure S108. χ_p•T plot *vs* T for melted **T[1]** after diamagnetic correction of χ_{dia} = -0.002750 cm^{3}mol^{-1} determined in Figure S107. The horizontal line marks the value of 0.375 Kcm^{3}mol^{-1} for an ideal paramagnet.

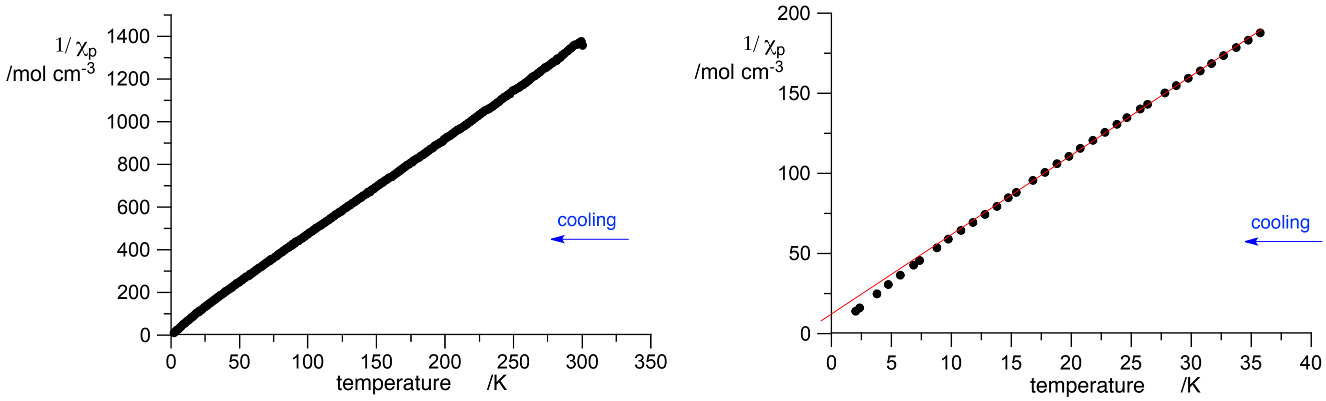

Figure S109. 1/χ_p plot *vs* T for melted **T[1]**. Best fit functions in the range 100–250 K:
1/χ_p = 30.1(4)+4.460(2)•T, r^2 = 0.9999.

Analysis of the 1/χ_p *vs* T plot for melted **T[1]** in Figure S109 according equation 2 gives the value C = 0.224 cm^{3}mol^{-1}K and the Weiss constant θ = –6.7 K.

Figure S110 shows total molar magnetization in function of applied field B, $M_{tot}(B)$ at selected temperatures.

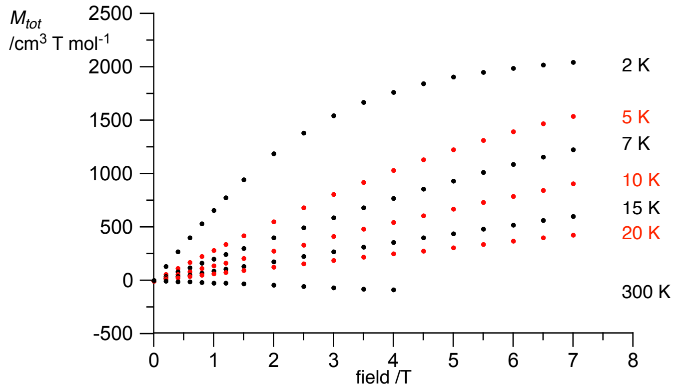

Figure S110. Molar total magnetization M_{mol} *vrs* field for melted **T[1]** at selected temperatures.

A comparison of χ_p•T (T) plots for pristine and melted samples of **T[1]** is shown in Figure S111.

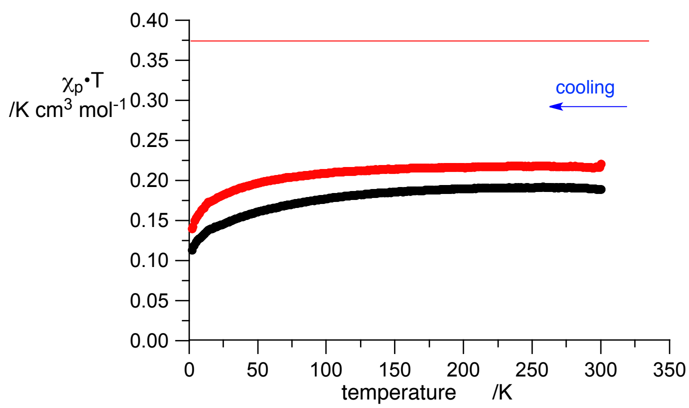

Figure S111. χ_p•T *vs* T plot for solid (black) and melted (red) sample of **T[1]** in the cooling mode. The horizontal line marks the value of 0.375 Kcm^{3}mol^{-1} for an ideal paramagnet.

Triradical **T[3]**. **pristine solid sample**

m = 14.92 mg, 9.724×10^{-6} mol/spin, M_w= 1534.37 g mol^{-1} per spin.

Total molar susceptibility, χ, of the sample as a function of temperature in the cooling mode is shown in Figure S112 and a χ•T *vs* T plot in Figure S113.

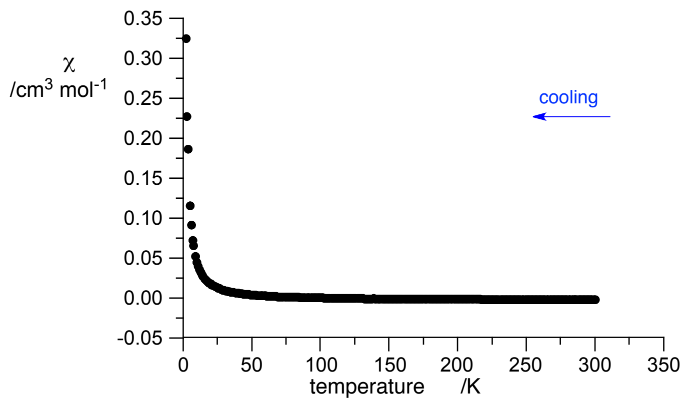

Figure S112. Molar magnetic susceptibility χ *vs* T obtained for solid **T[3]** on cooling 300 K → 2 K at 0.6 T. The cooling rate is 1 K/min.

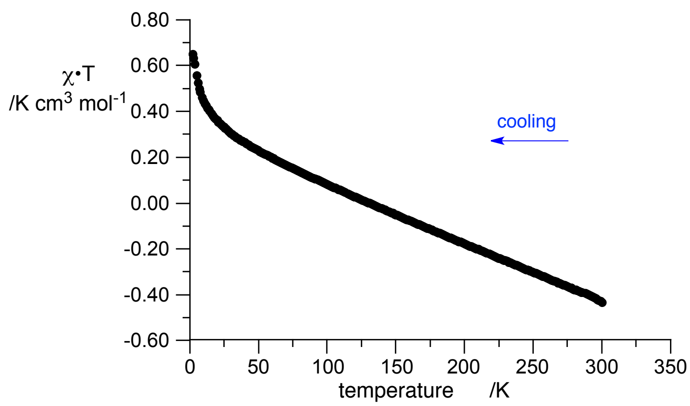

Figure S113. A χ•T *vs* T plot for solid **T[3]** obtained on cooling 300 K → 2 K at 0.6 T. The cooling rate is 1 K/min.

The diamagnetic correction, χ_{dia}, was determined from a linear portion of the χ•T *vs* T plot (Figure S113) in the temperature range 280 K – 200 K (Figure S114).

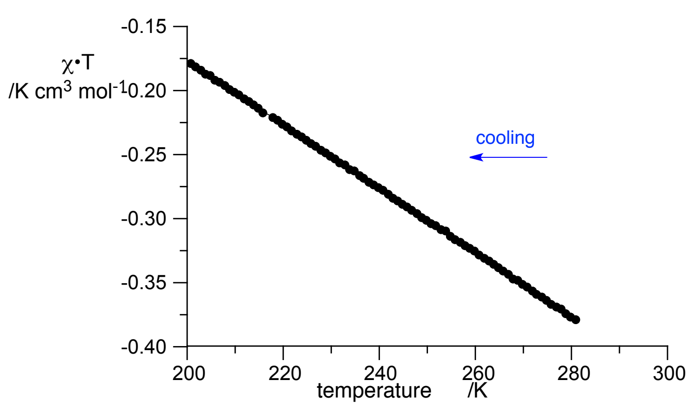

Figure S114. A linear portion of the χ•T *vs* T plot for solid **T[3]** (Figure S113) in the range of 280 K → 200 K. Best fit line: χ•T = -0.002493(2)•T + 0.32185(5), r^2 = 0.9999.

The diamagnetic correction of -0.002493•T $cm^3mol^{-1}K$ was applied to the χ•T plot and the resulting χ_p•T *vs* T plot is shown in Figure S115, while the $1/\chi_p$ *vs* T plot for solid **T[3]** is shown in Figure S116.

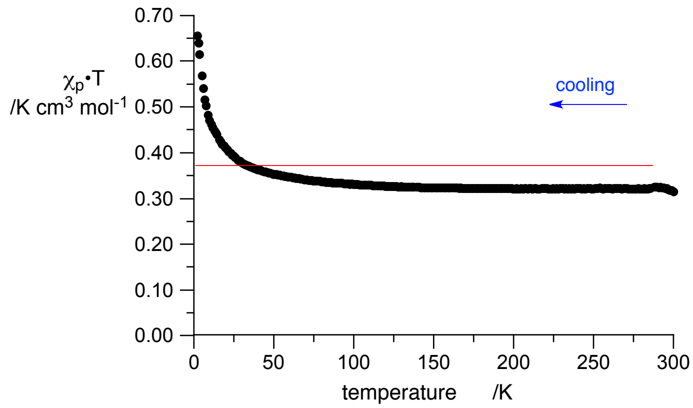

Figure S115. χ_p•T plot *vs* T for solid **T[3]** in the cooling mode after diamagnetic correction of χ_{dia} = -0.002493 cm^3mol^{-1} determined in Figure S114. The horizontal line marks the value of 0.375 Kcm^3mol^{-1} for an ideal paramagnet.

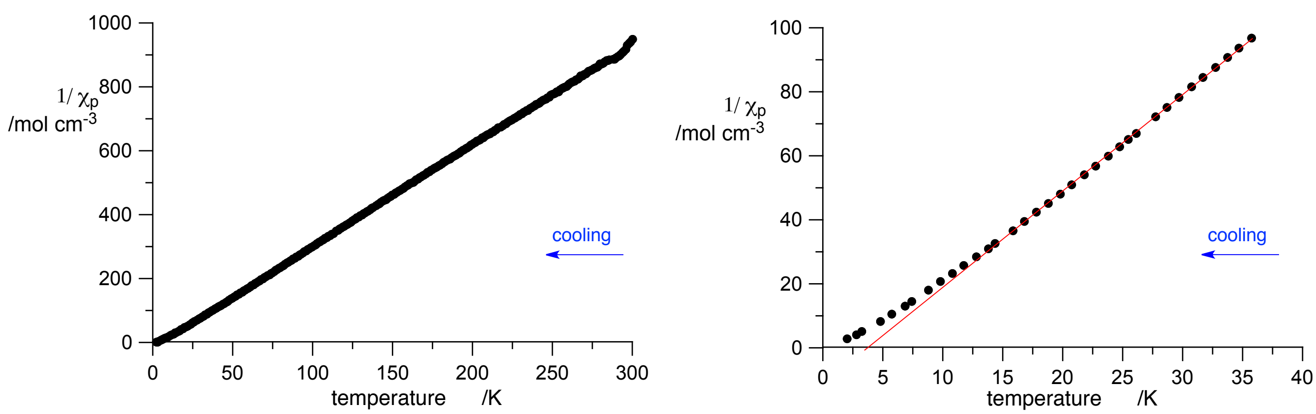

Figure S116. $1/\chi_p$ plot *vs* T for solid **T[3]** in the cooling mode. Best fit functions in the range 100–250 K: $1/\chi_p$ = -16.6(3)+3.186(2)•T, r^2 = 0.9999 for cooling.

Analysis of the $1/\chi_p$ *vs* T plot for solid **T[3]** according to equation 2 gives the value C = 0.314 $cm^3mol^{-1}K$ and the Weiss constant θ = +5.2 K.

The low temperature portion of the χ_pT(T) data (2–250 K) was fitted to Baker's high temperature series expansion function (equation 3b) using C = 0.314 $cm^3mol^{-1}K$ established in Curie-Weiss fitting (Figure S116). The results are shown in Figure S117.

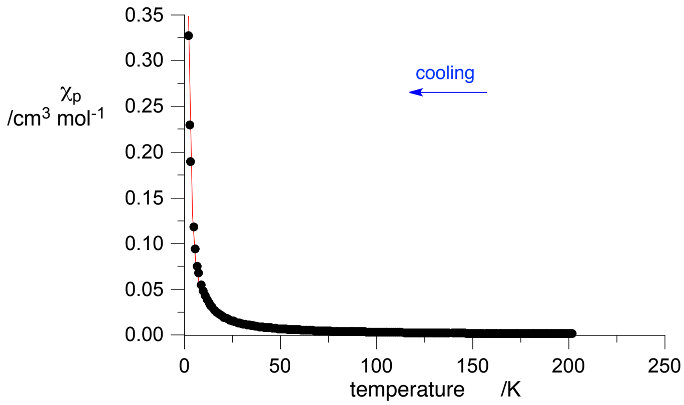

Figure S117. A χ_p *vs* T plot for solid **T[3]** in the cooling mode fitted to Baker's function with C = 0.314 cm^{3}mol^{-1}K (Figure S116). The best-fit functions give J/k_B = 3.04(4) K, r^2 = 0.993.

Figure S118 shows total molar magnetization in function of applied field B, $M_{tot}(B)$, in selected temperatures.

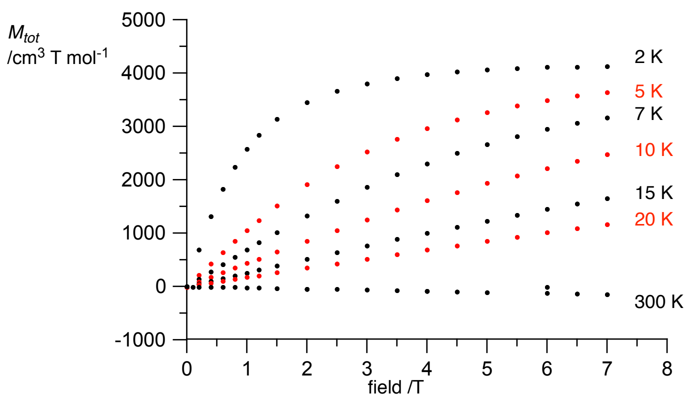

Figure S118. Molar total magnetization M_{mol} *vrs* field for solid **T[3]** at selected temperatures.

Triradical **T[3]**. **melted sample.**

A fresh sample of **T[3]** was briefly heated on a glass plate to *ca* 150 ºC, quickly cooled (quenched) and transferred to a polycarbonate capsule.

m = 7.53 mg, 4.908×10^{-6} mol/spin, M_w= 1534.37 g mol^{-1} per spin.

Total molar susceptibility, χ, of the melted sample as a function of temperature in the cooling mode is shown in Figure S119 and a χ•T *vs* T plot in Figure S120.

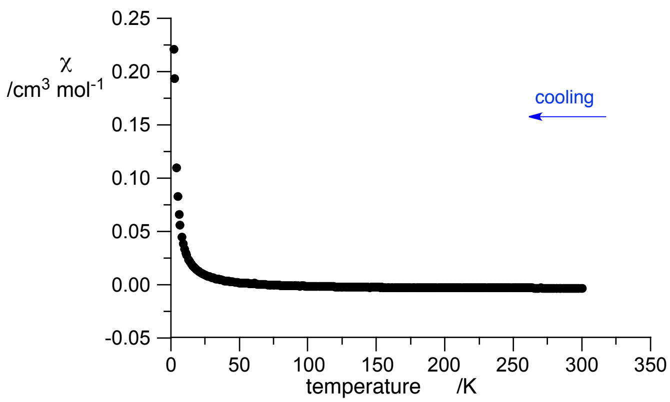

Figure S1189. Molar magnetic susceptibility χ *vs* T obtained for melted **T[3]** on cooling 300 K → 2 K at 0.6 T. The cooling rate is 1 K/min.

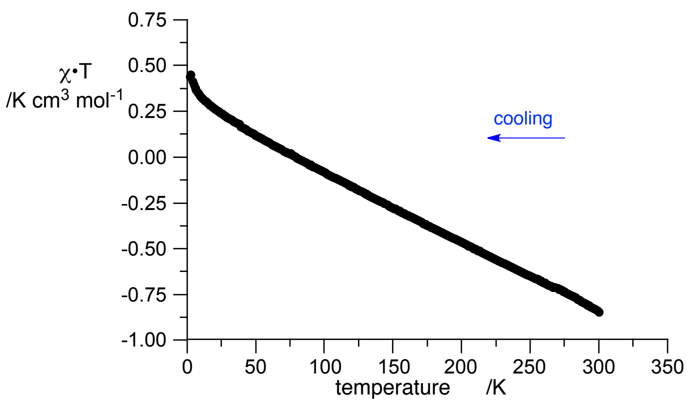

Figure S120. A χ•T *vs* T plot for melted **T[3]** obtained on cooling 300 K → 2 K at 0.6 T. The cooling rate is 1 K/min.

The diamagnetic correction, χ_{dia}, was determined from a linear portion of the χ•T *vs* T plot (Figure S120) in the temperature range 300 K – 200 K (Figure S121).

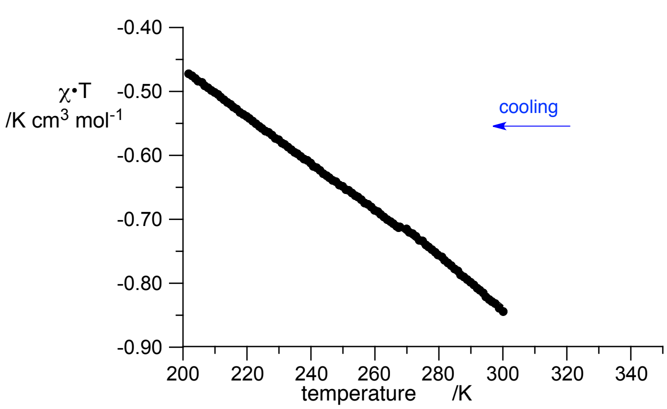

Figure S121. A linear portion of the χ•T *vs* T plot for melted **T[3]** (Figure S120) in the range of 200 K → 300 K. Best fit line: χ•T = -0.003684(11)•T + 0.272(3), r^2 = 0.9991.

The diamagnetic correction of -0.003684•T $cm^3mol^{-1}K$ was applied to the χ•T plot and the resulting χ_p•T *vs* T plot is shown in Figure S122, while the $1/\chi_p$ *vs* T plot for melted **T[3]** is shown in Figure S123.

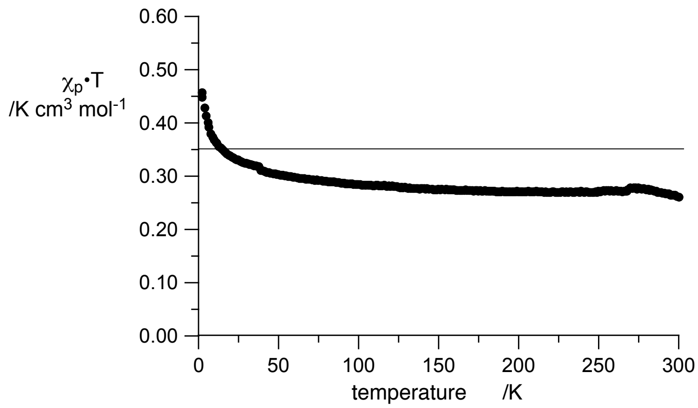

Figure S122. χ_p•T plot *vs* T for melted **T[3]** in the cooling mode after diamagnetic correction of χ_{dia} = -0.003684 cm^3mol^{-1} determined in Figure S121. The horizontal line marks the value of 0.375 Kcm^3mol^{-1} for an ideal paramagnet.

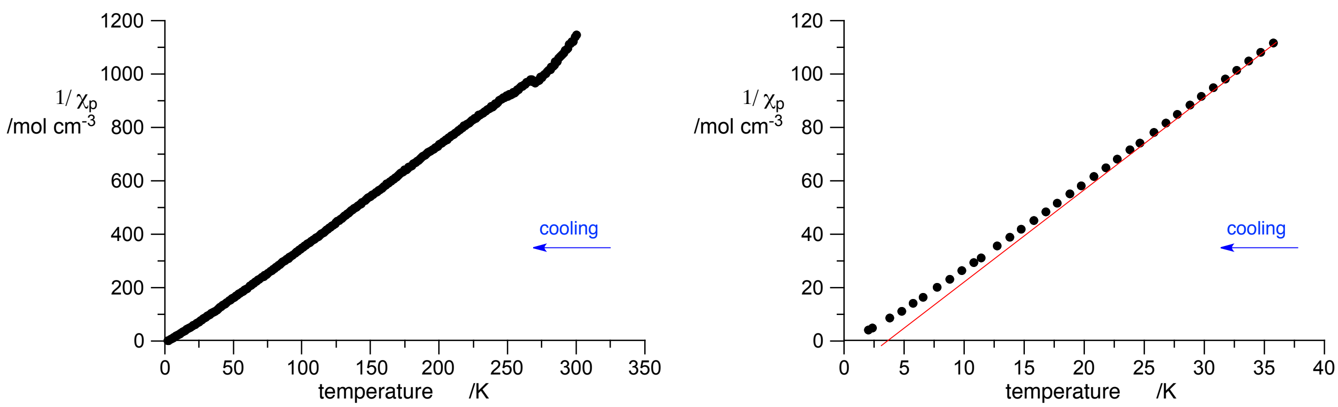

Figure S123. $1/\chi_p$ plot *vs* T for melted **T[3]** in the cooling mode. Best fit functions in the range 100–250 K: $1/\chi_p = -31.8(7)+3.834(4)$•T, $r^2 = 0.9998$.

Analysis of the $1/\chi_p$ *vs* T plot according to equation 2 gives the value $C = 0.261$ $cm^3mol^{-1}K$ and the Weiss constant $\theta = +8.3$ K.

The low temperature portion of the χ_pT(T) data (2–250 K, Figure S122) was fitted to Baker's high temperature series expansion function (equation 3b) using $C = 0.261$ $cm^3mol^{-1}K$ established in Curie-Weiss fitting (Figure S123). The results are shown in Figure S124.

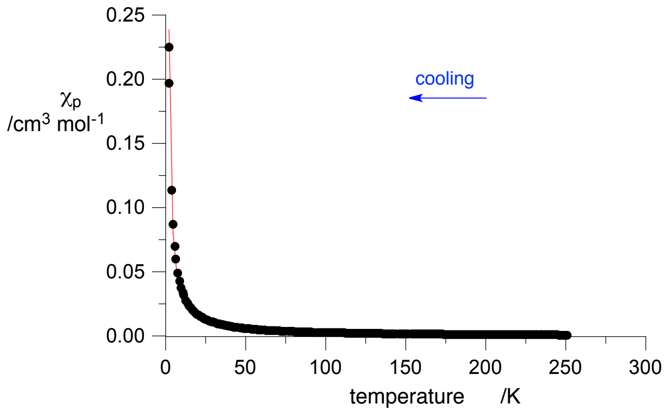

Figure S124. A χ_p *vs* T plot for melted **T[3]** in the cooling mode fitted to Baker's function with C = 0.261 $cm^3mol^{-1}K$ (Figure S123). The best-fit functions give J/k_B = 1.88(3) K, r^2 = 0.992.

Figure S125 shows total molar magnetization in function of applied field B, $M_{tot}(B)$, in selected temperatures, while A comparison of χ_p•T (T) plots for pristine and melted samples of **T[3]** is shown in Figure S126.

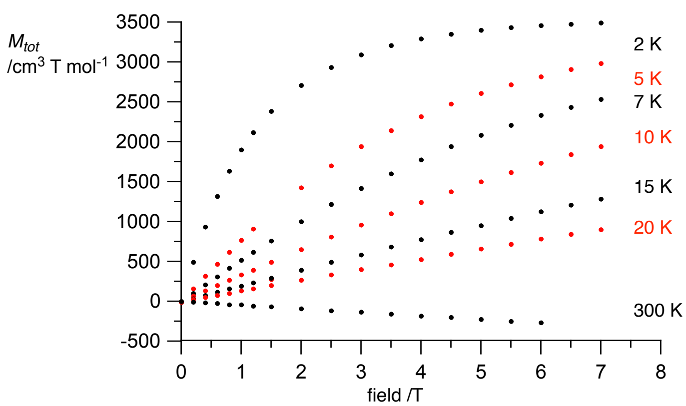

Figure S125. Molar total magnetization M_{mol} *vrs* field for melted **T[3]** at selected temperatures.

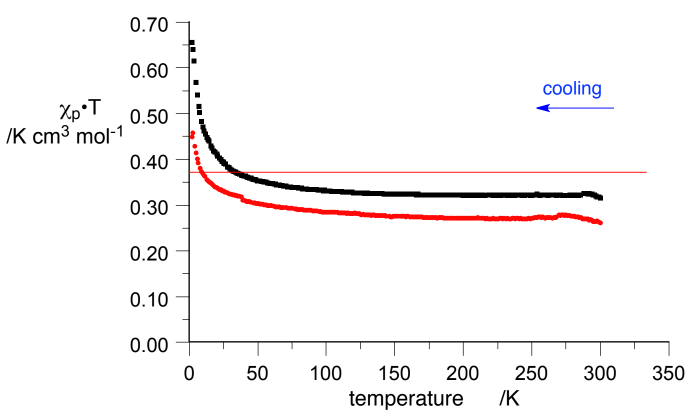

Figure S126. χ_p•T *vs* T plots for solid (black) and melted (red) sample of **T[3]** in the cooling mode. The horizontal line marks the value of 0.375 Kcm^3mol^{-1} for an ideal paramagnet.

Triradical **T[6]**. **pristine solid sample**

m = 12.12 mg, 7.899×10^{-6} mol/spin, M_w= 1534.37 g mol^{-1} per spin.

Total molar susceptibility, χ, of the sample as a function of temperature in the cooling mode is shown in Figure S127 and a χ•T *vs* T plot in Figure S128.

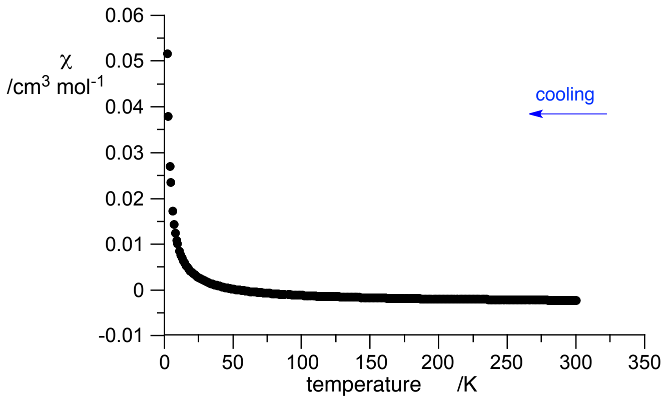

Figure S127. Molar magnetic susceptibility χ *vs* T obtained for solid **T[6]** on cooling 300 K → 2 K at 0.6 T. The cooling rate is 1 K/min.

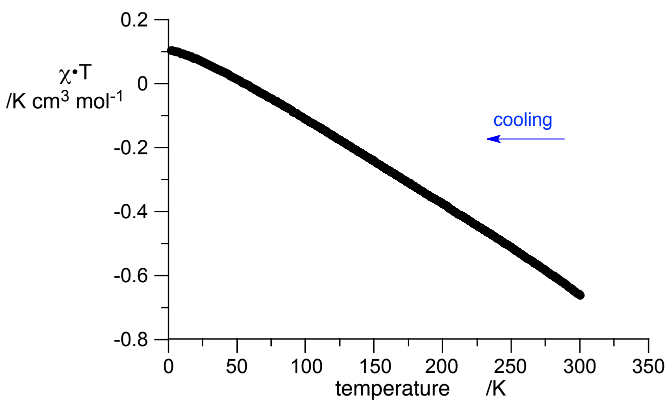

Figure S128. A χ•T *vs* T plot for solid **T[6]** obtained on cooling 300 K → 2 K at 0.6 T. The cooling rate is 1 K/min.

The diamagnetic correction, χ_{dia}, was determined from a linear portion of the χ•T *vs* T plot (Figure S128) in the temperature range 300 K – 270 K (Figure S129).

The diamagnetic correction of -0.003038•T cm^{3}mol^{-1}K was applied to the χ•T plot and the resulting χ_p•T *vs* T plot is shown in Figure S130, while the 1/χ_p *vs* T plot in Figure S131.

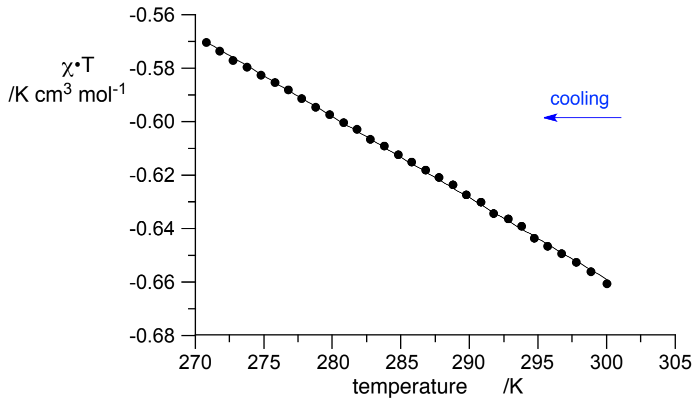

Figure S129. A linear portion of the χ•T *vs* T plot for solid **T[6]** (Figure S128) in the range of 270 K → 300 K. Best fit line: χ•T = -0.003038(14)•T + 0.253(2), r^2 = 0.9994.

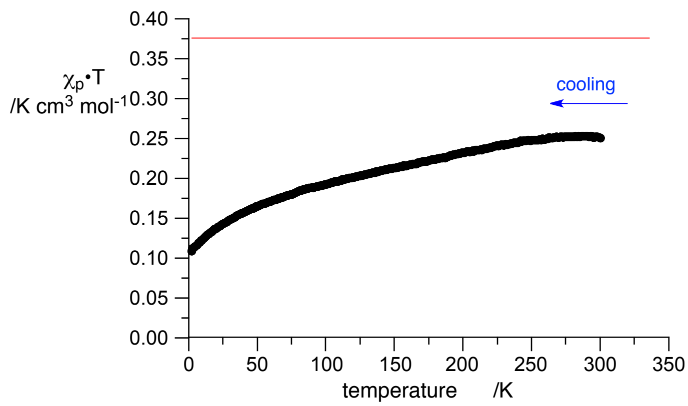

Figure S130. χ_p•T plot *vs* T for solid **T[6]** in the cooling mode after diamagnetic correction of χ_{dia} = -0.003038 cm^3mol^{-1} determined in Figure S129. The horizontal line marks the value of 0.375 Kcm^3mol^{-1} for an ideal paramagnet.

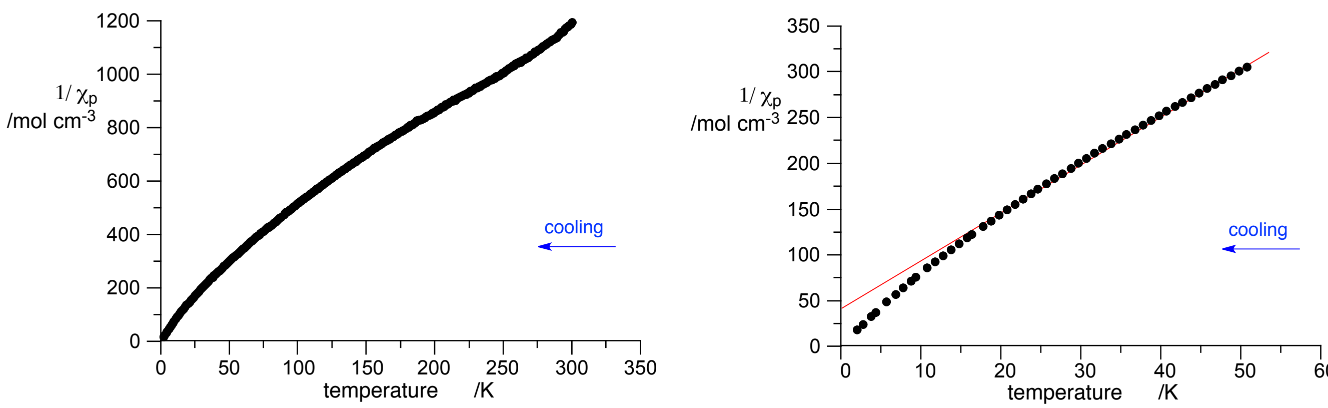

Figure S131. 1/χ_p plot *vs* T for solid **T[6]** in the cooling mode. Best fit function in the range 150–250 K: 1/χ_p = 261(2)+2.99(1)•T, r^2 = 0.9990.

Analysis of the $1/\chi_p$ *vs* T plot according to equation 2 gives the value C = 0.334 $cm^3 mol^{-1}K$ and the Weiss constant $\theta = -87$ K.

Figure S132 shows total molar magnetization in function of applied field B, $M_{tot}(B)$, in selected temperatures.

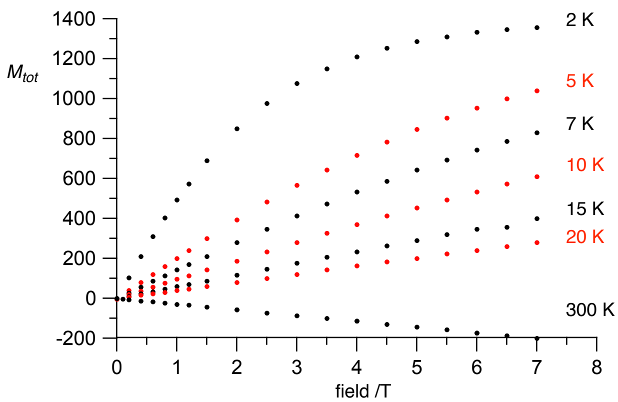

Figure S132. Molar total magnetization M_{mol} *vrs* field for solid **T[6]** at selected temperatures.

Triradical **T[6]**. **melted sample**

A fresh sample of **T[6]** was briefly heated on a glass plate to *ca* 150 °C, quickly cooled (quenched) and transferred to a polycarbonate capsule.

m = 9.34 mg, 6.087×10^{-6} mol/spin, M_w= 1534.37 g mol^{-1} per spin.

Total molar susceptibility, χ, of the melted sample as a function of temperature in the cooling mode is shown in Figure S133 and a χ•T *vs* T plot in Figure S134.

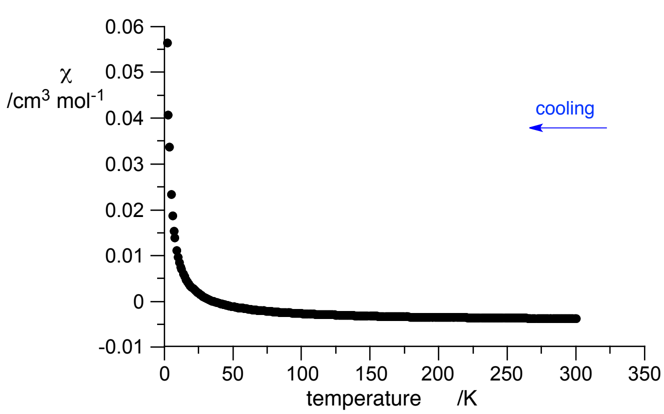

Figure S133. Molar magnetic susceptibility χ *vs* T obtained for melted **T[6]** on cooling 300 K → 2 K at 0.6 T. The cooling rate is 1 K/min.

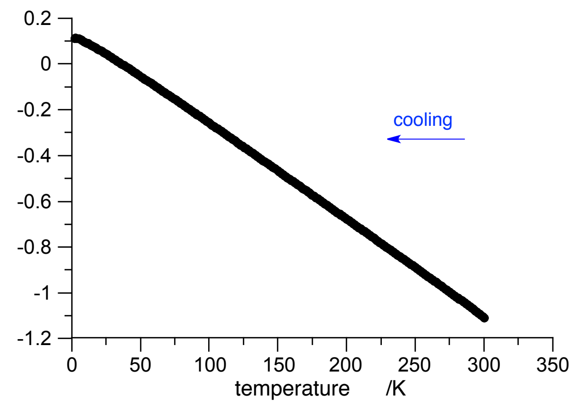

Figure S134. A χ•T *vs* T plot for melted **T[6]** obtained on cooling 300 K → 2 K at 0.6 T. The cooling rate is 1 K/min.

The diamagnetic correction, χ_{dia}, was determined from a linear portion of the χ•T *vs* T plot (Figure S134) in the temperature range 300 K – 200 K (Figure S135).

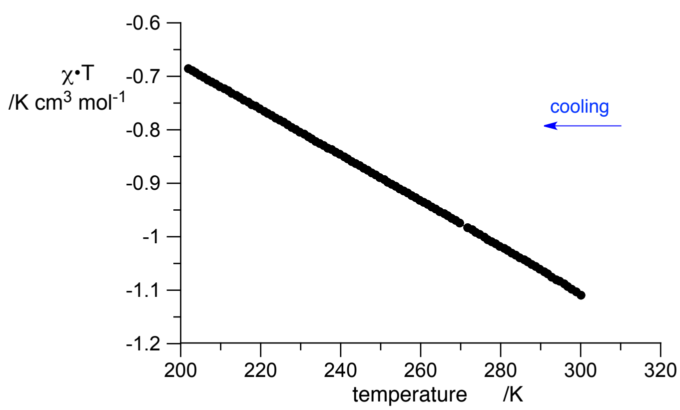

Figure S135. A linear portion of the χ•T *vs* T plot for melted **T[6]** (Figure S134) in a range of 300 K → 200 K. Best fit line: χ•T = -0.004277(4)•T + 0.1795(9), r^2 = 0.9999.

The diamagnetic correction of -0.004277•T $cm^3mol^{-1}K$ was applied to the χ•T plot and the resulting χ_p•T *vs* T plot is shown in Figure S136, while the 1/χ_p *vs* T plot in Figure S137.

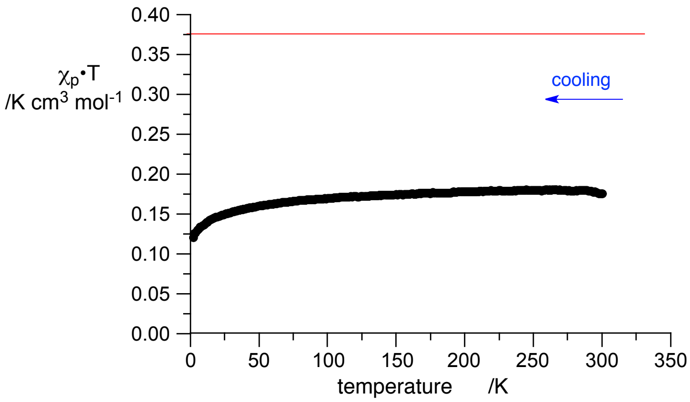

Figure S136. χ_p•T plot *vs* T for melted **T[6]** in the cooling mode after diamagnetic correction of χ_{dia} = -0.004277 cm^3mol^{-1} determined in Figure S135. The horizontal line marks the value of 0.375 Kcm^3mol^{-1} for an ideal paramagnet.

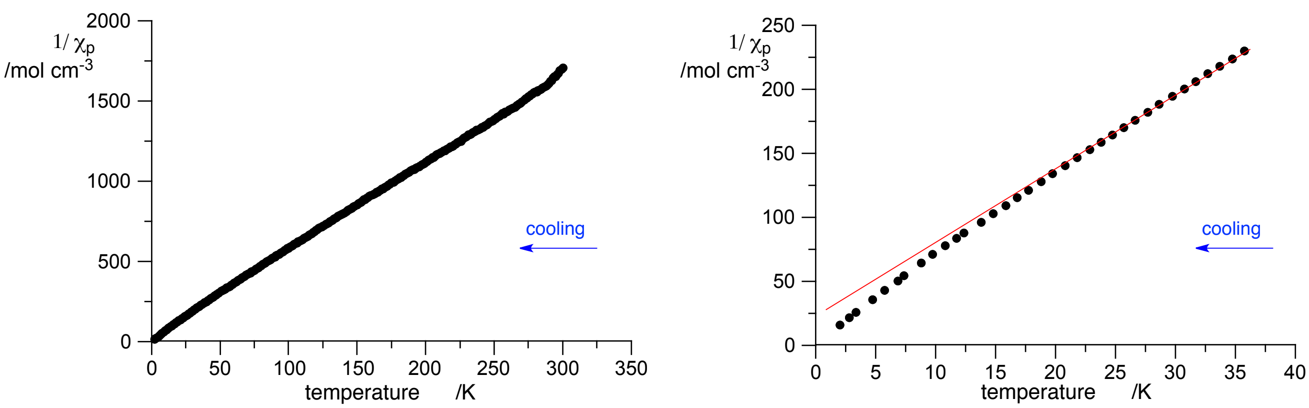

Figure S137. 1/χ_p plot *vs* T for melted **T[6]** in the cooling mode. Best fit functions in the range 100–250 K: 1/χ_p = 60.6(8)+5.307(5)•T, r^2 = 0.9999 for cooling.

Analysis of the 1/χ_p *vs* T plot for melted **T[6]** according to equation 2 gives the value C = 0.188 $cm^3mol^{-1}K$ and the Weiss constant $\theta = -11.4$ K.

Figure S138 shows total molar magnetization in function of applied field, $M_{tot}(B)$ at selected temperatures.

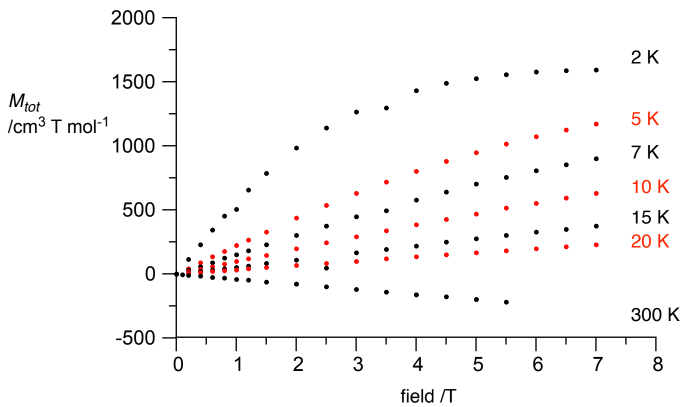

Figure S138. Molar total magnetization M_{mol} *vrs* field for melted **T[6]** at selected temperatures.

A comparison of χ_p•T (T) plots for pristine and melted samples of **T[6]** is shown in Figure S139.

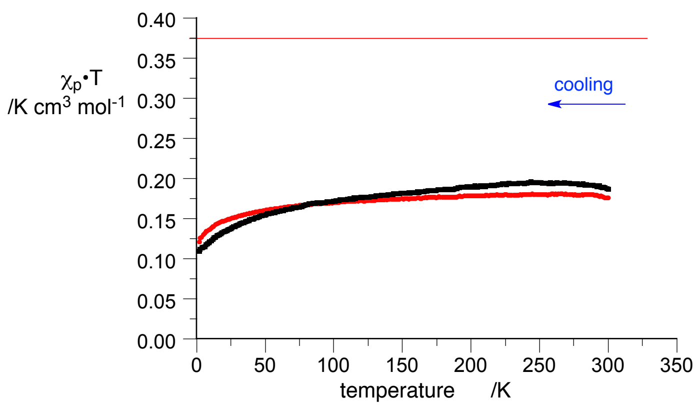

Figure S139. χ_p•T *vs* T plots for solid (black) and melted (red) sample of **T[6]** in the cooling mode. The horizontal line marks the value of 0.375 Kcm^{3}mol^{-1} for an ideal paramagnet.

5.2. Variable temperature EPR measurements

Temperature dependent EPR spectra for **B[n]**, **T[n]** and **3[1]** were obtained using an X-band Nano- EMX Bruker EPR spectrometer. The compound (about 0.5 mg) was contained within the BRAND® disposable BLAUBRAND® micropipettes, intraMark (green color coded) capillaries to a height of about 0.5 cm and were not degassed. The heating cycle for **B[n]**, **T[n]** and **3[1]** was carried out in the range 240–430 K with tolerance and interval set to 4 and 5 K, respectively. A total number of points were collected allowing for 20 s of temperature stabilization at each point. The cooling cycle for these radicals was carried out in a range of 430–240 K with the tolerance and interval set to 5 and 5 K, respectively. A total number of points were collected, allowing for 20 s of temperature stabilization at each point. The microwave power was optimized at different level of attenuation to avoid signal saturation and the EPR signals were collected at 25 dB. Center Field was set at 3444.0 G and Sweep width for 200 G. The line width was measured as a difference in position of the maximum and minimum of the EPR signal. The *g* value was red directly from the spectra. The spin count was obtained by double integration of the region of the EPR signal from the signal onset till its termination.

An example of EPR signal dependence on temperature is shown in Figure S140.

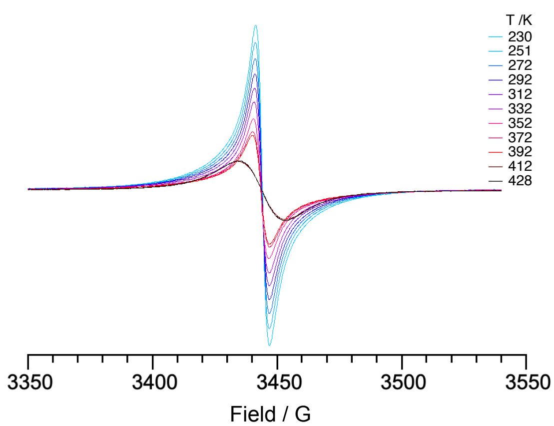

Figure S140. Temperature dependence of the EPR curve shape upon heating of **B[3]** powder sample in the range of 230 – 428 K.

6. References

1. M. Jasinski, J. Szczytko, D. Pociecha, H. Monobe and P. Kaszyński, Substituent-dependent magnetic behavior of discotic benzo[*e*][1,2,4]triazinyls, *J. Am. Chem Soc.*, 2016, **138**, 9421−9424.
2. S. Kapuściński, A. Gardias, D. Pociecha, M. Jasiński, J. Szczytko and P. Kaszyński, Magnetic behaviour of bent-core mesogens derived from the 1,4-dihydrobenzo[*e*][1,2,4]triazin-4-yl, *J. Mater. Chem. C*, 2018, **6**, 3079-3088.

3. M. Jasinski, K. Szymańska, A. Gardias, D. Pociecha, H. Monobe, J. Szczytko and P. Kaszyński, Tuning magnetic properties of columnar benzo[*e*][1,2,4]triazin-4-yls with the molecular shape, *ChemPhysChem*, 2019, **20**, 636–644.
4. G. A. Baker, Jr., G. S. Rushbrooke and H. E. Gilbert, High-Temperature Series Expansions for the Spin 1/2 Heisenberg Model by the Method of Irreducible Representations of the Symmetric Group, *Phys. Rev.*, 1964, **135**, A1272–A1277.